C.P No 144
(15,144)
A R.C. Technical Report

MINISTRY OF SUPPLY

AERONAUTICAL RESEARCH COUNCIL

CURRENT PAPERS

The Performance of the 108 Compressor Fitted with Low Stagger Free Vortex Blading

By

D. V. Foster

LONDON : HER MAJESTY'S STATIONERY OFFICE

1954

Price 3s 6d net

C.P. No.144

Report No.116

June, 1952

NATIONAL GAS TURBINE ESTABLISHMENT

The Performance of the 108 Compressor Fitted with Low Stagger Free Vortex Blading

- By -

D. V. Foster

SUMMARY

This report contains a description of a large three-stage compressor which has been designed for detail three dimensional flow investigations. Particular attention has been paid to the accuracy of measurement on the rig and it is shown that the main errors are due to the unsteady nature of the flow and to speed fluctuations. Both of these factors are, however, considerably less than those normally experienced on compressor test work.

The test characteristics of the first set of low stagger free vortex blading are presented and compared with various theoretical performance calculations. Discrepancies between the theoretical and experimental characteristics are attributed to low deviations, and to very little degeneration of the axial velocity profile. Some miscellaneous results, including a description of the surging behaviour of the compressor and the effect of blade position upon the measured static pressure are also given.

CONTENTS

		Page
1.0	Introduction	4
2.0	The apparatus	4
2.1	The compressor	4
2.2	Compressor instrumentation	5
2.3	Outlet ducting	6
2.4	The throttle	6
2.5	The drive	6
3.0	Measurements	7
3.1	Input power and speed	7
3.2	Pressure rise	8
3.3	Mass flow	8
4.0	Design of first set of blading	10
5.0	Test results	10
5.1	The overall and stage characteristics with inlet guide vanes	10
5.2	Performance without inlet guide vanes at the design flow coefficient	11
5.3	Off design performance without inlet guide vanes	12
6.0	The influence of blade position on static pressure measurement	12
7.0	The behaviour of the compressor when surged	12
7.1	Observed flow	12
7.2	The characteristics when surged	13
8.0	Conclusions	14
References		15
Appendix I	Compressor geometry and blade inspection	17
Appendix II	Calculation and accuracy of non-dimensional coefficients.	19

ILLUSTRATIONS

Fig. No.	Title	Sk. or Neg. No.
1	External Side View of Compressor	Neg. Rep/28/52
2	Layout of Compressor	Sk. 55149
3	View during erection showing Stator Traversing Ring	Neg. Rep/29/52
4	Pitot Comb and Traverse Gear	Neg. Rep/30/52
5	Outlet Ducting Arrangement	Sk. 55150
6	Scatter of Compressor Static Pressure Readings	Sk. 17127
7	Venturimeter Velocity Profile	Sk. 17136
8	Venturimeter Axial Static Pressure Distribution	Sk. 17136
9	Mean Stage Characteristics with Inlet Guide Vanes	Sk. 53260
10	Stage Static Pressure Rise Characteristics with Inlet Guide Vanes	Sk. 53263
11	Stator Outlet Angles at Design Point	Sk. 17110
12	Compressor Outlet Velocity Profile	Sk. 17110
13	Mean Stage Characteristics without Inlet Guide Vanes	Sk. 53261
14	Stage Static Pressure Rise Characteristics without Inlet Guide Vanes	Sk. 53262
15	Radial Equilibrium Velocity Profiles between Blade Rows	Sk. 17128
16	Variation of Measured Static Pressure with Blade Position	Sk. 17109
17	Distribution of Static Pressure Rise between Blade Rows when Surged	Sk. 55267
18	Overall Characteristics Measured at the end of the Diffuser	Sk. 17135

1.0 Introduction

Although the secondary flow in cascades is fairly well understood, little is known about the more complex secondary flows which occur in axial compressors and turbines. These flows result in a considerable difference between the actual performance and that calculated from two dimensional cascade data, and account for about half the total losses occurring in compressors.

These secondary flows have been described by various authors[1,2,3] and include:-

(i) The shed vorticity resulting from variations of circulation along the blade, either by design or due to the velocity profile.

(ii) Velocities associated with the radial pressure gradients.

(iii) Tip clearance and shroud ring leakages.

(iv) Flows resulting from the relative movement of the inner and outer annulus walls.

(v) Possible rotor and stator interference effects.

In order to make a detailed investigation of these secondary effects a large scale compressor and its associated equipment have been built. A turbine similar to the compressor and to be driven by it, is also under construction.

This report describes the compressor and its equipment, and the methods of making the various measurements. The accuracy of these measurements is also considered, particular attention being paid to the calibration of the venturi meter. Some results of a preliminary nature are presented including the overall and stage characteristics which are compared with various theoretical estimates of performance. The influence of blade position on static pressure measurement and the behaviour of the compressor when surged have also been examined.

2.0 The apparatus

2.1 The compressor

The main design considerations were that the compressor should be fully instrumentated, of convenient size and power, and corresponding in diameter ratio and aspect ratio to the middle stages of conventional compressors.

A large blade chord was desirable

(i) to reduce the power needed to obtain full scale Reynolds Number

(ii) to permit the use of instruments which are small compared with the region being investigated, but large enough to avoid sluggishness and difficulty in manufacture.

(iii) to measure blade static pressure distributions, since the pressure tappings have to be taken out along the blade through hypodermic tubing which must be of reasonable size to avoid sluggishness.

An aspect ratio of two and a diameter ratio of 0.7 were considered representative. A convenient blade chord was about three inches, which gave a blade height of six inches, and inside and outside diameters of twenty eight and forty inches respectively. The axial pitching of the blade rows is four inches or one and one third blade chords so that the axial blade row separation is rather greater than a third of a chord, thus allowing ample room for traversing instruments.

In order to examine the effect of an axial velocity profile after it has developed appreciably, there are three stages of geometrically similar blading, there being a negligible density change through the compressor. Full scale Reynolds number of 3×10^5 occurs at about 1000 r.p.m. The horse-power under these conditions for conventional blading will be about one hundred, which will result in a torque of about five hundred foot-pounds, both of which are of convenient magnitude to supply and measure with commercially available equipment. An external side view of the compressor is shown in Fig. 1.

In order to avoid interference from the wakes of spiders, an over-hung construction was used as shown in Figs. 2 and 3, and since there are only three stages and the speed is low it was convenient to use a drum construction with the support bearing in a cone protruding within the drum. Thus the bearing nearest the rotor was close to the rotor centre of gravity and the whirling speed was greatly increased compared with a more conventional design. The construction is mainly of light alloy, the rotor being cast aluminium alloy and in three sections. Both rotor and stator blades are slotted in peripheral grooves, thus allowing variations of pitch and relative blade positions in adjacent rows.

2.2 Compressor instrumentation

The compressor is at present equipped to investigate the airflow between the blade rows and the stator blade static pressure distributions. It is hoped to provide later for static pressure measurements on the rotor blades and possibly traversing of the stator blade passages.

Traversing the instruments between and relative to the blade rows is obtained by rotation of the stator blade holding rings to obtain peripheral movement. Fig. 2 shows these stator rings. The rigidly mounted instrument carriage provides radial traversing and rotates the instrument for yaw measurement. Each of the stator blade holding rings rolls upon the outer races of four single row ball bearings held by their centre races and is actuated by a worm which meshes with a worm wheel cut on the outside of the stator blade holding ring. The position of the stator blade is indicated by a graduated dial attached to the worm shaft.

The instrument carriage is shown in Fig. 4 and can be fitted into any of six equally spaced bosses which are provided on the stator casing between each pair of blade rows. A dowel peg located in the boss prevents rotation of the traverse gear and also serves to fix the zero for yaw measurement. The yaw measurement of the traverse gear is made backlash free by spring loading the worm, which actuates the yaw measurement, into the worm wheel and fixing the exploring instrument to a square cast iron rod. This slides radially in a Vee slot into which it is pressed by a phosphor bronze leaf spring. Radial movement is obtained by a pinion acting on a rack cut on the inside edge of the cast iron rod, and radial position is measured by means of a scale on the outside edge of the rod which is viewed through a slot in the phosphor bronze leaf spring. A vernier scale is engraved on the side of the slot in the leaf spring.

2.3 Outlet ducting

In order to extend the flow range to include low pressure rises at high mass flows it is essential that as much of the outlet velocity as possible be recovered in a diffuser. This is the purpose of the outlet ducting, which also incorporates an airflow measuring venturimeter and the throttle. A longitudinal section through it is shown in Fig. 5.

Immediately following the compressor there is an annular diffuser of approximately eight degrees equivalent cone angle which has eight aerofoil section spiders to support the central cone, and with blading having outlet swirl these would exert a considerable straightening effect since their pitch-chord ratio is low. The diffuser outlet diameter is 50 inches and it is immediately followed by a straightening gauze having about two velocity heads pressure drop.

After the gauze there is a settling length one diameter long in which a honeycomb straightener of 10 inches axial length and having one inch square passages can be placed if the compressor has a high outlet whirl. This is followed by the venturimeter contraction which is a sine curve, a convenient shape which avoids excessive curvature and changes of slope. The venturi throat is twenty eight inches in diameter and is fabricated from one eighth inch thick plate. Static holes were made in it by screwing in brass inserts which are smoothed off on the inside. The throat velocity head is diffused through an eight degree conical diffuser up to the entrance to the throttle.

2.4 The throttle

The outlet throttle is shown in Fig. 5 and combines the advantage of being an efficient diffuser when open with that of discharging normal to the axis of the compressor. This was necessary since the axial length available was limited.

The centre conical part of this annular throttle is made of wood with a large tapped brass insert at the centre which moves on a substantial steel shaft having a square thread cut on it which mates with the brass nut. The throttle is actuated by a hand wheel attached to the end of the shaft, the hand wheel also acting as a fine position indicator by moving over a graduated circle behind it. The coarse position of the throttle is read directly from a scale alongside the moving centre cone and attached to the fixed metal outer part of the throttle, thus the exit area of the throttle was directly proportional to the throttle position given by these readings and, as described in 3.3, this was used in conjunction with the throttle pressure drop to measure the airflow at low flows and high pressure rises.

2.5 The drive

The compressor is driven by an electric motor which is swung to allow direct measurement of the driving torque. The driving motor is a level compound direct current shunt motor supplied by a motor generator set with Ward-Leonard control which permits continuous speed variation from zero to top speed. The motor is swung by the end-shields, as shown in Figs. 1 and 3, in double row self aligning ball races. About seven balls in each bearing are touching both races at a given time. It is shown in 3.1 that the shaft rotates about its geometric centre, at least for the small angular movement involved in weighing the torque with the stiff weighing machine used and subject to the small vibration present when running.

The motor is swung with the feet in a vertical plane as shown in Figs. 1 and 2. The torque on the motor frame is transmitted to the springless type of weighing machine through knife edges which are attached to a short steel bar which protrudes horizontally from the motor lifting eye socket. The main armature and the field currents for the motor are supplied through mercury pots directly beneath the motor axis, thus avoiding buoyancy effects on the torque measurement, due to the slight movement when weighing.

A small gear box is incorporated in the outer motor end shield from which two drives are taken for speed measurement. Since the speed measuring devices are fixed to the motor and not the support, the power consumption is automatically subtracted from the motor output and no correction to the measured torque is necessary.

3.0 Measurements

3.1 Input power and speed

Since the maximum temperature rise of the compressor is only three degrees centigrade and the air is discharged into the room, the variations of inlet temperature are of this order. Thus it is not convenient to measure the temperature rise directly and it must be calculated from the input power and mass flow.

The method of torque measurement has been indicated in Section 2.5 and it requires the accurate measurement of the effective torque arm and the calibration of the weighing machine. The weighing machine is of the direct reading dial type and it was checked with known weights over its full range of 400 lb., and no error greater than one fifth of a pound could be found.

The torque arm was measured directly, assuming rotations about the centre of the shaft as 22.02 inches with an error of about $\pm$ 0.01 inches. In order to check this value and to determine whether the motor was rotating about the centre of the bearing, or possibly about each of the ball bearings in turn, the effective torque arm was found indirectly. Another torque arm was fixed on the opposite side of the motor and weights attached to knife edges fixed to it. Hence, from the measured distance between the two sets of knife edges and the ratio of the weights and the weighing machine readings, the effective torque arm and point of suspension could be found. The mean torque arm found from four such tests was 22.030 inches and the average deviation from the mean of the four tests was 0.015 inches. Hence this value is probably accurate to better than one part in a thousand. These tests covered different ranges of the weighing machine and the motor was run at the same time to provide a slight vibration, such as occurs during normal running, in order to remove any tendency to stickiness.

The input torque to the compressor is then obtained as the difference between the measured torque and the torque at the same speed when the motor is uncoupled. This latter is not zero owing to the motor windage and frictional effects which are, however, small. The moving parts of the weighing machine are protected from the motor cooling draught.

The speed is measured by two instruments attached to the two shafts of the motor end shield gear box. One is an indicating tachometer of the conventional aircraft type which is used to observe any variations of speed, for setting the speed and keeping it constant. The other is a direct counting instrument which gives the mean speed over the period of a test. This consists

of a commutator in series with a battery and an electrical pulse counter, the circuit being electrically interlocked with another circuit which starts and stops a stop-watch. By this means the average speed over an interval can be found to any desired degree of accuracy, 2000 revolutions being normally counted, with a corresponding accuracy of one part in a thousand.

Although the mean speed can be accurately determined, variations in speed are equally important since these affect the other measurements which are being taken. This is one of the main sources of error. It is of the order of a quarter of one per cent at the top speed and becomes more serious as the speed decreases. It is hoped to reduce this effect at the lower speeds by an electronic speed regulator attached to the Ward-Leonard set.

3.2 Pressure rise

The static pressure between each blade row is measured at twelve points around the circumference. These are spaced equally except for two which are slightly offset due to the split in the casing. Thus, when the number of blades is a multiple of twelve, ten static holes are similarly placed with respect to blades. This is the case with the present set of blades which have a pitch-chord ratio of about 0.75 at the mean diameter. It will be seen from a later section that the static pressure field of the blades is appreciable at the static hole position, and it follows that errors will be introduced by variations in blade pitching and static hole position.

The static holes are each 0.052 inches in diameter and are drilled in the bottom of brass tubes which convey the pressure through the double casing and the gap between. The ends of the tubes are smoothed off flush with the inside of the casing.

In addition to the static holes on the outer casing there are four more on the inner casing at the inlet just before the rotor drum and opposite to the row before the inlet guide vanes. There is a difference of about 10% x $\frac{1}{2}\rho V_a^2$ between these two static pressures due to the bend of the annulus at the inlet, the pressure on the outer wall static being lower. Thus the intake efficiency calculated from the outer static is low and inaccurate.

In order to determine if there was any systematic peripheral variation of static pressure throughout the compressor, the variation from the mean at each blade row is plotted against position round the circumference in Fig. 6. No systematic circumferential variation is apparent and from the analysis of these results the "standard error" of the mean static pressure at each row is about 0.4% x $\frac{1}{2}\rho V_a^2$. These static pressures were instantaneously observed, no attempt being made to average the indicated pressure over a period of time.

Total head pressures are measured with combs of total head tubes which can be inserted in the holes provided for the exploring instruments and some are shown in Fig. 4. Each comb has one tube at the middle of the annulus and one $\frac{1}{4}$, $\frac{1}{2}$, 1 and $1\frac{1}{2}$ inches from each wall making nine tubes in all.

3.3 Mass flow

It is desirable that any mass flow measuring devices shall be at the compressor outlet to avoid interference with the inlet velocity profile. Hence a venturimeter, which combines the advantage of direct calibration by traversing with a low pressure loss, is placed in the outlet ducting. The throttle is also calibrated for mass flow in terms of pressure drop and opening. This is used at low flows when the throttle pressure drop is high while that across the venturimeter is relatively low.

A longitudinal section of the venturimeter and the adjacent ducting is shown in Fig. 5. Since the area of the venturi throat is approximately equal to that of the compressor annulus and the diameter ratio of the venturi is large it is convenient to calibrate the venturimeter by expressing the compressor axial velocity head in terms of the venturi pressure drop.

A convenient expression is:-

$$(\tfrac{1}{2}\rho\bar{V}_a^2) \text{ compressor outlet} = K\Delta p \ (1 - k\Delta p)$$

where Δp is the venturi pressure drop and K and k are constants.

Δp is measured between static holes in the venturi throat and a section just before the contraction by means of a Betz manometer. The actual static hole pressures used need not be accurately representative of conditions at the cross sections considered but must be consistent since Δp must be proportional to the compressor outlet velocity head for incompressible flow without losses.

k is a small, but not negligible, factor for taking compressibility into account by means of a parabolic approximation and for allowing for pressure losses between the compressor outlet and the venturi throat. That part of k which is due to compressibility is calculated from the cross sectional area of the various portions of the duct; while that due to losses in the outlet ducting and gauze is calculated from experimentally measured losses.

K incorporates the velocity of approach factor, venturi discharge coefficient and the effect of the ratio of the compressor annulus area to the venturi throat area. It is found by maintaining Δp constant and determining $\frac{1}{2}\bar{V}_a^2$ at the compressor outlet from the flow measured at the venturi throat. To determine this flow it is necessary to know the distribution of total head and static pressure in the throat. The total head pressure distribution was found by traversing the throat with a pitot tube which projected about three inches upstream of the aerofoil section tubing to which it was attached in order to avoid interference with the boundary layer profile. Two perpendicular diameters were traversed and the profile is shown in Fig. 7. The variations between profiles were small compared with the variations in the mean profile. Some trouble was experienced at first due to gradual clogging of the gauze resulting in a change of the throat total head profile but this was cured by fitting a coarser gauze of one quarter inch clear mesh woven from one eighth inch diameter stainless wire.

The throat static pressure was measured at eight positions round the circumference at the traversing section, and its variation along the wall of the throat was found from four rows of four tappings. Each of the static tappings was 0.030 inches in diameter and smooth on the inside. The throat assembly was tested for leaks by covering it with a medium oil when the internal pressure was above atmospheric. The static pressure distribution along the throat axis was determined by means of a half inch diameter static tube which projected in front of the throat so that the contraction would stabilise the boundary layer. This axial static pressure distribution is plotted in Fig. 8 together with the peripheral variation at the traverse section which shows a slight systematic variation. The static pressure on the axis is seen to be about 0.8% x $\frac{1}{2}\rho\bar{V}_a^2$ greater than the value at the outside wall or, since the maximum will occur at the centre, the value at the area mean diameter is about 0.4% x $\frac{1}{2}\rho V_a^2$. Hence the effect on $\frac{\bar{V}_a}{U_m}$ and the efficiency will amount to about 0.2%, and will be such as to reduce the mass flow and increase the efficiency. The mass flow is also reduced by about 0.2% due to the humidity. This was assumed constant since any error due to its variation was necessarily small.

The outlet throttle was calibrated by plotting:-

$$\frac{\text{Compressor outlet velocity head}}{\text{Throttle pressure drop}}^{\frac{1}{2}}$$

against throttle position. This gave a straight line with some scatter at very low flows, where the venturi measurement was relatively inaccurate. From this mean line and knowing the throttle pressure drop and position the compressor outlet velocity head was obtained.

4.0 Design of first set of blading

The first set of blading is low stagger, the flow coefficient being 0.8 at the mean diameter where the rotor and stator design air outlet angles are 24.6 and 3.4 degrees respectively. The design temperature rise coefficient at mean diameter was 1.0, where the pitch-chord ratio of both rotor and stator is 0.742. The blades were twisted to make the whirl velocities inversely proportional to the radius (free vortex flow), with 50% reaction at the inside diameter.

These air angles were to be obtained from constant 10% thick C4 section blading on a parabolic camber line having the position of maximum camber 40% of the chord from the leading edge. Both the design and measured blade angles and details of the compressor dimensions are given in Appendix I. Since the flow is virtually incompressible, the blading in each stage is the same.

The predicted temperature rise coefficient was based on an assumed work done factor of 0.86, deduced from multi-stage compressor test results[4]. Present methods of performance estimation employ work done factors of 0.98, 0.93, 0.88 for the first three stages respectively and thereafter for the remaining stages a constant value of 0.835. Thus the mean value for ten stages is 0.86 and for three, 0.93, and the predicted temperature rise for this three stage compressor would be correspondingly higher.

The design of the rig and the first set of blading were completed several years ago. It is not representative of contemporary designs which have higher staggers and generally employ circular arc camber lines. It is not thought that the low stagger design will detract from the value of three dimensional flow investigations on this blading.

5.0 Test results

5.1 The overall and stage characteristics with inlet guide vanes

The mean stage characteristics, plotted as temperature rise coefficient $\frac{J_0 \Delta T}{\frac{1}{2}U_m^2}$; pressure rise coefficient $\frac{\Delta p}{\frac{1}{2}\rho U_m^2}$; and efficiency, (the ratio of these two); against flow coefficient, $\frac{\overline{V}_a}{U_m}$, are given in Fig. 9. The characteristics are given for speeds of 900, 700 and 500 r.p.m., corresponding to mean stage Reynolds numbers based on the inlet velocity and blade chord of 2.8, 2.2, and 1.6×10^5 respectively at the design flow coefficient of 0.8. These coefficients include the compressor bearing and drum windage losses and are based on the static pressure rise. Since the overall pressure rises at 900, 700 and 500 r.p.m. are approximately 12, 7 and $3\frac{1}{2}$ inches of water, the changes in $\frac{1}{2}\rho\overline{V}_a^2$ through the compressor are about 2,1 and $\frac{1}{2}$% respectively. The total head pressure rises and efficiencies will be correspondingly lower than the static values.

It is seen that Reynolds number has little effect on the temperature rise, that is the outlet angle, for the Reynolds number investigated. The effect on the losses, and hence the efficiency and pressure rise, is appreciable however, and thus the effect of Reynolds number is similar to that previously observed at the N.G.T.E. and reported in Ref. (6). The corresponding peak total head efficiency at the highest Reynolds number was 88.5%, including bearing and windage losses.

The characteristics calculated by means of Ref. (4) are also plotted on Fig. 9, work done factors of 0.98, 0.93 and 0.88 being assumed for the first, second and third stages respectively. The main difference between the calculated and experimental characteristics is the greater observed work capacity of the blading, the discrepancy increasing as the flow increases. The high efficiency range of the compressor is also much greater than calculated. The surged characteristics are also given for the lowest speed, but were not repeated at higher speeds where the blade stresses, which are not known, would be higher. It is not expected that the surge flow will vary much with Reynolds number since the flow is very turbulent.

The stage pressure rise characteristics are plotted in Fig. 10 and it is clear from these that at the design flow coefficient of 0.8 the first stage is doing considerably less work than the other two. This is contrary to expectation, since, due to degeneration of the velocity profile, the work done and pressure rise are normally greatest in the first stage of compressors.

Since the work done in the last two stages was so great that it could not be accounted for, even by a work done factor of unity, the stator fluid outlet angles were measured at the mean diameter and the traverses are shown in Fig. 11. Clearly the mean stator fluid outlet angle was approximately zero compared with a cascade value interpolated from Ref. (8), of 1.5°, which is also in agreement with Ref. (9). The outlet angle from the inlet guide vanes was correct and hence the first stage was doing considerably less work than the other two.

5.2 Performance without inlet guide vanes at the design flow coefficient

In order to attempt to match the first stage to the other two, the inlet guide vanes were removed and the compressor re-tested. The overall and stage characteristics of the compressor in this state are shown in Figs. 13 and 14 respectively. The stage pressure rises are now seen to be almost equal at the design flow coefficient of 0.8.

The stage performance does not deteriorate through the compressor, as is normally the case due to degeneration of the velocity profile. To investigate this the outlet velocity profile was obtained and is plotted in Fig. 12. It is seen to be very flat, and this lack of degeneration is thought to be due to good flow conditions at the blade ends. These include the good inlet velocity profile, resulting in the incidences being near design and little reduction in Reynolds number occurring near the blade ends. The blade thickness is constant along the blade height and equal to 10%, a value close to the optimum from the incidence range point of view. Since the design is free vortex, adverse incidences will not result from changes in the axial velocity profile necessary to satisfy radial equilibrium. Also the Mach numbers are so low as to be negligible. The blade root fillets and tip clearances are also favourable. This lack of degeneration has been observed previously on the similar but rather higher stagger, compressor of Ref. (10).

5.3 Off-design performance without inlet guide vanes

Off design the stage static pressure rise characteristics differ considerably in slope and have been little changed in this respect by the removal of the inlet guide vanes. In order to determine if this could be accounted for by the velocity profile changing so as to satisfy radial equilibrium, the performance was calculated assuming radial equilibrium to be satisfied between the blade rows by the method given in Ref. (11). The stator outlet angle was taken to be zero and the rotor outlet angles to be given by

$$\tan\alpha_2 = 0.0735r - \frac{13.39}{r}$$

where r is the radius in inches. Thus the flow is free vortex when the flow coefficient $\frac{V_a}{U_m} = 0.80$.

The calculated axial velocity profiles at four flow coefficients are shown in Fig. 15, from which it is clear that the axial velocity at the mean diameter is close to the mean axial velocity. Since the stator outlet angle is zero, and there can thus be no radial pressure gradients, the calculated stage static pressure rises at the outside diameter are about equal to that calculated on mean diameter conditions and using the mean axial velocity. Hence the stage performances calculated on this basis, which are plotted in Fig. 14, are approximately equal and radial equilibrium cannot explain the different performances.

As when the inlet guide vanes were in, the high efficiency part of the characteristic is very wide. This is very likely associated with the failure of the velocity profile to degenerate which, it was pointed out in Section 5.3, was connected with favourable flow conditions near the blade ends resulting in low secondary losses.

6.0 The influence of blade position on static pressure measurement

It was found that varying the position of the stator blade affected the static pressure measurement both before and after the stator blade rows. Some traverses are shown in Fig. 16 from which it is seen that the variation amounts to about ± 7% of the stage rise at design point. The static holes were two-thirds of a blade chord behind the centre of the blade rows. The effect would probably diminish rapidly if this distance were increased.

It is seen that the traverses after the blade row intersect in an approximately fixed position about 1% below zero which is useful for obtaining stage characteristics. Whether this effect is entirely due to the blade static pressure field or to the root fillets is not known but further information would seem desirable and could be obtained from a cascade tunnel.

Provided the static holes are in the same position relative to blades in each stage, this effect will cancel out except for the first stage.

7.0 The behaviour of the compressor when surged

7.1 Observed flow

As on most medium and low stagger compressors of conventional diameter ratio, when the throttle is closed there comes a point close to the peak pressure rise when the nature of the flow suddenly changes accompanied by a reduction of pressure rise. The flow is then of a periodic nature which is

usually known as surging. The flow in this compressor near the inlet has been examined when the compressor was in this state by means of wool tufts and consists of a single rotating band having reverse flow at the outside of the annulus but inward flow at the inside. That there was only one band, was confirmed by the static pressure distribution round the circumference since when any row of static tappings are connected in order to adjacent manometers a single wave is seen to travel across in the direction of rotation. That the flow as a whole was not pulsating was confirmed by the steady driving torque.

The flow remains similar as the throttle is further closed, the blow-back occupying rather more of the cycle. If the throttle is opened past a certain point the flow changes again and moves up towards the main characteristic but can remain at an intermediate point. If the throttle is then closed it will follow out a short rising characteristic before the flow changes once more to that of the main surged characteristic. The backward flow on the short surge line is similar at all radii and the pulse appears to be steeper and shorter than that of the main surge as if two or three blade passages were completely blown back. This appears to be confirmed by observation with wool tufts.

The frequencies of the surges are given in the following table as a percentage of the rotor speed. They did not vary with mass flow or speed.

	Main	Minor
With inlet guide vanes	32.1	42.8
Without inlet guide vanes	40.6	50.9

7.2 The characteristics when surged

The over-all surged characteristics are given in Fig. 18. The beginnings and ends of the characteristics, including the main, are not definite points but very short regions of instability. If the compressor is started from rest when the throttle is in such a position that it is possible for the compressor to run surged at that setting, then it will run on the major surged characteristic.

Although the input power is steady, when the compressor is surged, the pressures are fluctuating and the coefficients plotted are based upon observed mean values. The manometer fluctuations were small compared with the pressure rise due to the high damping in the pressure measuring system. The static pressure oscillations after the last stator have been measured with the piezo electric manometer of Ref. (12) and are between $1\frac{1}{2}$ and 2 times $\frac{1}{2}\rho U_m^2$ for both surges. The pressure rise can be measured directly, without trouble due to the fluctuations, by means of a U-tube manometer connected to equiphase points in the various rows of static holes.

The high efficiency (70%) of the short (minor) surge is surprising and the distribution of pressure rise among the stages given in Fig. 17 is seen to be almost normal. It would appear therefore that little air is blowing back or else the backward flow is of high efficiency. A high efficiency seems most unlikely since the gas angles are most unfavourable and the sharp trailing edges and low reaction of the stator blades would almost certainly lead to breakaway with a corresponding low efficiency. As mentioned in 7.1 observations indicate that there is relatively little backflow through two or three passages only.

The pressure rise of the forward flowing air will be given by the pressure rise above atmospheric at the end of the annular diffuser, neglecting intake and diffuser losses and the small velocity head at this section. Such characteristics for the compressor with the inlet guide vanes in are given in Fig. 18. The pressure rise characteristic of the minor surge is seen to have a negative slope, indicating that the forward flowing air is restricted to a definite flow area and in consequence the axial velocity is reduced and the pressure rise increases when the throttle is closed. The pressure rise characteristic of the main surge is flat which confirms the observation that the change in nett through-put is obtained by varying the percentage of the annulus blown back, the velocities and gas angles apparently remaining unaltered. The slight fall in pressure rise at very low mass flows is attributed to the warming up of the air in the compressor.

8.0 Conclusions

(1) The compressor is satisfactory for the purpose for which it was designed, that is the detailed investigation of the airflow within a compressor. It is also suitable for the accurate measurement of overall performance, the mass flow, work input and mean speed being accurately known but the instantaneous speed and the static pressure rise are rather less accurate.

(2) Static pressure measurements are greatly affected by static hole position and a number of holes spaced over a blade pitch appear desirable to obtain reasonable accuracy in the first stage characteristic. The effect will cancel out in the other stages provided the static holes are in the same position relative to blades. The effect might be due to the blades or the fillets and could be investigated on a cascade tunnel.

(3) The deviations at mean diameter are lower than those of two-dimensional flow. This results in an increased work capacity and, if the inlet guide vanes give the two dimensional outlet angle, a first stage characteristic different from those of the other stages. This has been observed on other compressors.

(4) Contrary to general experience the velocity profile does not degenerate rapidly. The same feature has however been observed in another large experimental compressor. This is probably due to favourable flow conditions near the blade ends. It results in high work done factors in the later stages.

(5) The high efficiency is maintained over a wide range of mass flow. It is thought that the good velocity profile is responsible for this.

(6) The steepness of the first stage static pressure rise characteristic measured at the outside diameter is attributed to the axial velocity profile not having reached its form for radial equilibrium at the static hole position, one sixth of a chord behind the blade row.

(7) In consequence of (3), (4), (5) and (6), the usual stage by stage calculations of Ref. (4) and (7) greatly underestimate the on and off design performance.

(8) When the compressor is surged there is a single rotating band of reversed flow. It is believed that on the short surge line there is a small number of blade passages completely blown back and on the main surge the blow back is at the outside diameter and extends over a number of passages. The air flowing through the compressor during the main surge always has the same pressure rise whereas on the minor surge it follows a rising characteristic as the flow is reduced.

REFERENCES

No.	Author	Title
1	A. R. Howell	"Fluid Dynamics of Axial Compressors". Proceedings of the Institution of Mechanical Engineers. Vol. 153 (1945) p.448.
2	A. D. S. Carter	"Three Dimensional Flow Theories for Axial Compressors and Turbines". N.G.T.E. Report No. R.37. Proceedings of the Institution of Mechanical Engineers. Vol. 159 (1948) p.255.
3	D. G. Ainley	"Performance of Axial Flow Turbines". N.G.T.E. Report No. R.38. Proceedings of the Institution of Mechanical Engineers. Vol. 159 (1948) p.230.
4	A. R. Howell	"The Present Basis of Axial Compressor Design" Part 2 - Compressor Theory and Performance. R.A.E. Report No. E.3961 (1942).
5	A. R. Howell and R. P. Bonham	"Overall and Stage Characteristics of Axial-Flow Compressors". Proceedings of the Institution of Mechanical Engineers. Vol. 163 (1950) p.239.
6	R. A. Jeffs	"Preliminary note on the performance of Axial Compressor Blading Designed to Operate in a Radially Varying Axial Velocity Distribution". A.R.C.12,623. August, 1949.
7	A. R. Howell	"The Present Basis of Axial Compressor Design". Part 1 - "Cascade Theory and Performance". R & M 2095 (1942).
8	P. J. Fletcher	"Low Speed Tests on Compressor Cascades of Parabolic Aerofoils". Part 2 - "Pitch chord Ratio 0.75". (Unpublished).
9	A. D. S. Carter	"The Low Speed Performance of Related Aerofoils in Cascade". C.P.29. September, 1949.
10	J. T. Bowen, R. H. Sabersky and W. D. Rannie	"Investigations of Axial Flow Compressors". Transactions A.S.M.E. January, 1951.
11	H. Cohen and Elizabeth M. White	"The Theoretical Determination of the Three-dimensional Flow in an Axial Compressor with Special Reference to Constant Reaction Blading". A.R.C.6842. 1943.
12	W. Merchant, J. T. Hansford and P. M. Harrison	"The Flow of an ideal fluid in an annulus". Metropolitan Vickers Report.

REFERENCES (Cont'd)

No.	Author	Title
13	F. E. Marble	"The Flow of a perfect fluid through a Turbomachine with prescribed blade loading". Journal of the Aeronautical Sciences. August, 1948.
14	P. J. Fletcher	"A Three Channel Piezo Electric Pressure Recorder". C.P.35. November, 1949.
15	S. Gray	"The Fluid Dynamic Notation in Current Use at N.G.T.E. C.P.97. July, 1950.
16	D. G. Ainley and R. A. Jeffs	"Analysis of the Air Flow through Four Stages of Half Vortex Blading". R. & M.2383. April, 1946.

APPENDIX I

Compressor Geometry and Blade Inspection

Inside diameter = 28 in.)
Outside diameter = 40 in.) I.D./O.D. = 0.7

Blade height = 6 in.)
Blade chord = 3 in.) Height/Chord = 2.0

48 blades per row $\therefore$ s/c = 0.874 O.D.
= 0.742 M.D.
= 0.611 I.D.

Distance apart of blade rows - centre to centre = 4 in. = $1\frac{1}{3}$ chords
Blade base profile = C4 Ref. (15)
The blade thickness-chord ratio was constant and = 10%
Camber line - Parabolic Arc a/c = 40%
Rotor and stator tip clearances = 0.040 in. $\pm$ 0.010 in.
= 0.7% blade height.

Blade inspection

All the stator blades and rotor blades were to the same design and two of each of the inlet guide vanes, rotor blades and stator blades were inspected by projecting a ten times full size image together with the blade base datum for determining the stagger. This was done at five sections, these being the tip, middle and half an inch from the root, together with halfway between these positions.

The method of determining the blade outlet angles was to put in the camber line, measure the maximum camber and, assuming a/c = 0.4, calculate χ_1 and χ_2. The method of drawing tangents to the camber line was tried but found to be inconsistent and inaccurate.

The mean angles are tabulated on page 18.

In addition to this the projections were compared with drawings on the same scale and the blades examined to see that they were of good shape and accuracy.

A fillet of 1/2 in. radius extended round the blade root.

Rewriting this expression as:-

$$\frac{Kp.\Delta T}{\frac{1}{2}U_m^2} = \frac{W \times \text{Constant}}{\left\{\frac{1}{2}\rho 8 V_a^2 8 . \frac{1}{2}\rho o U_m\right\}^{1/2}}$$

where suffix 8 refers to the compressor outlet. The error can be seen to consist of 1/4% due to $\frac{1}{2}\rho 8 V^2 a 8$, 0.1% due to U_m and about 1/4% due to fluctuations in the indicated weight. Combining these and bearing in mind that they are independent, the accuracy of the flow coefficient will be about 0.4%.

Since the Mach number is low and never exceeds 0.23 at the mean diameter, any variation in the characteristics with speed will, after allowing for bearing and windage losses, be attributable to Reynolds number effects.

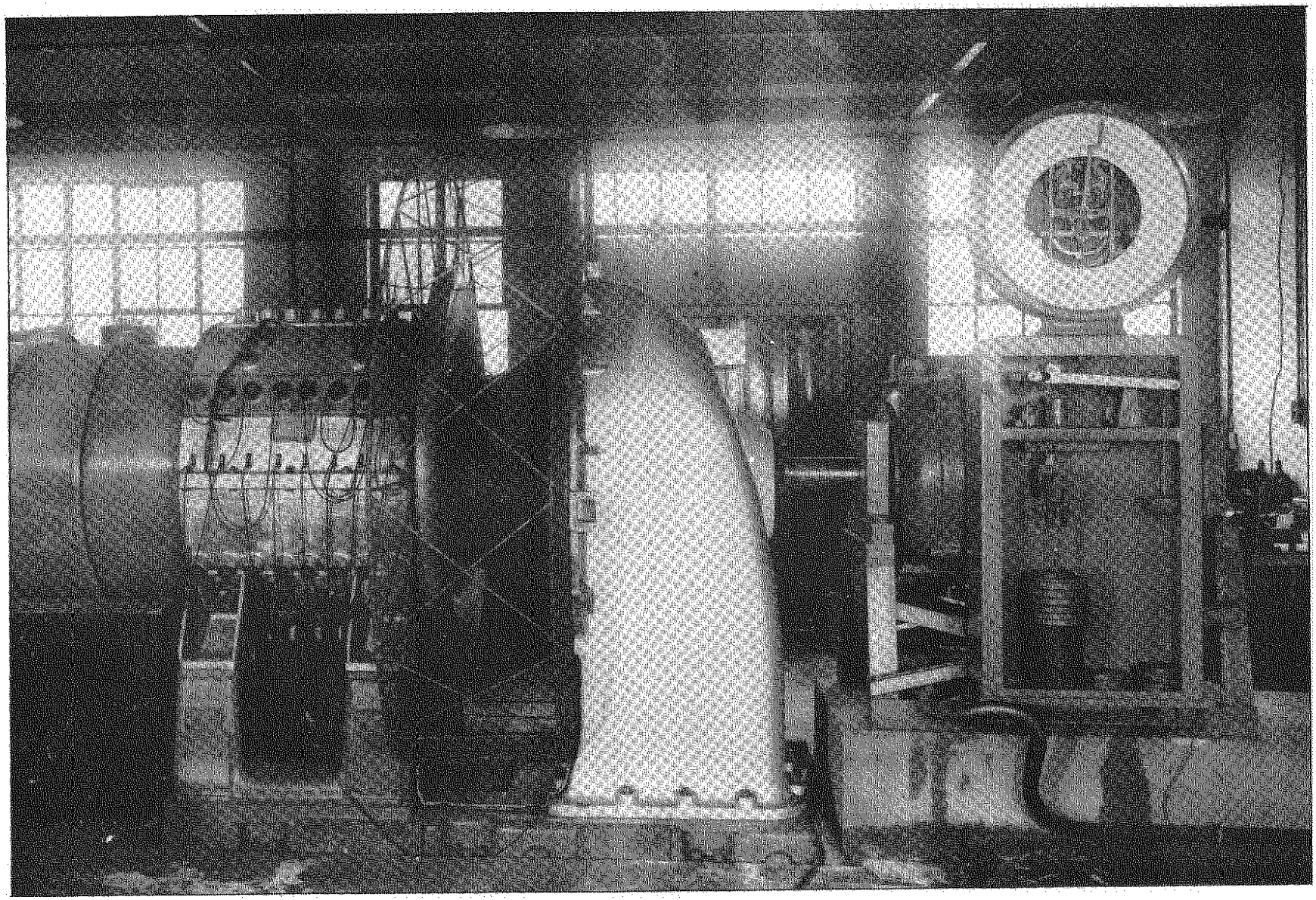

EXTERNAL VIEW OF 108 COMPRESSOR.

FIG.1

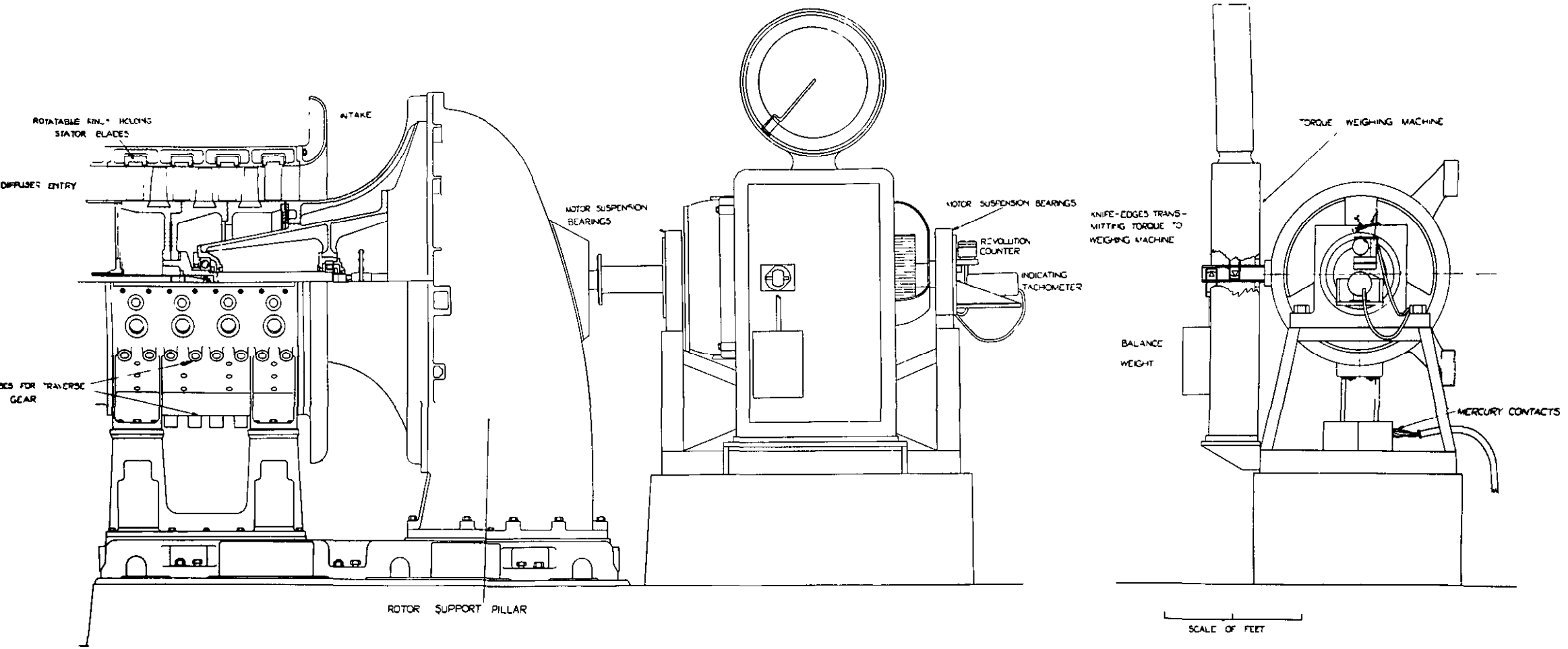

LAYOUT OF 108 COMPRESSOR.

FIG. 2

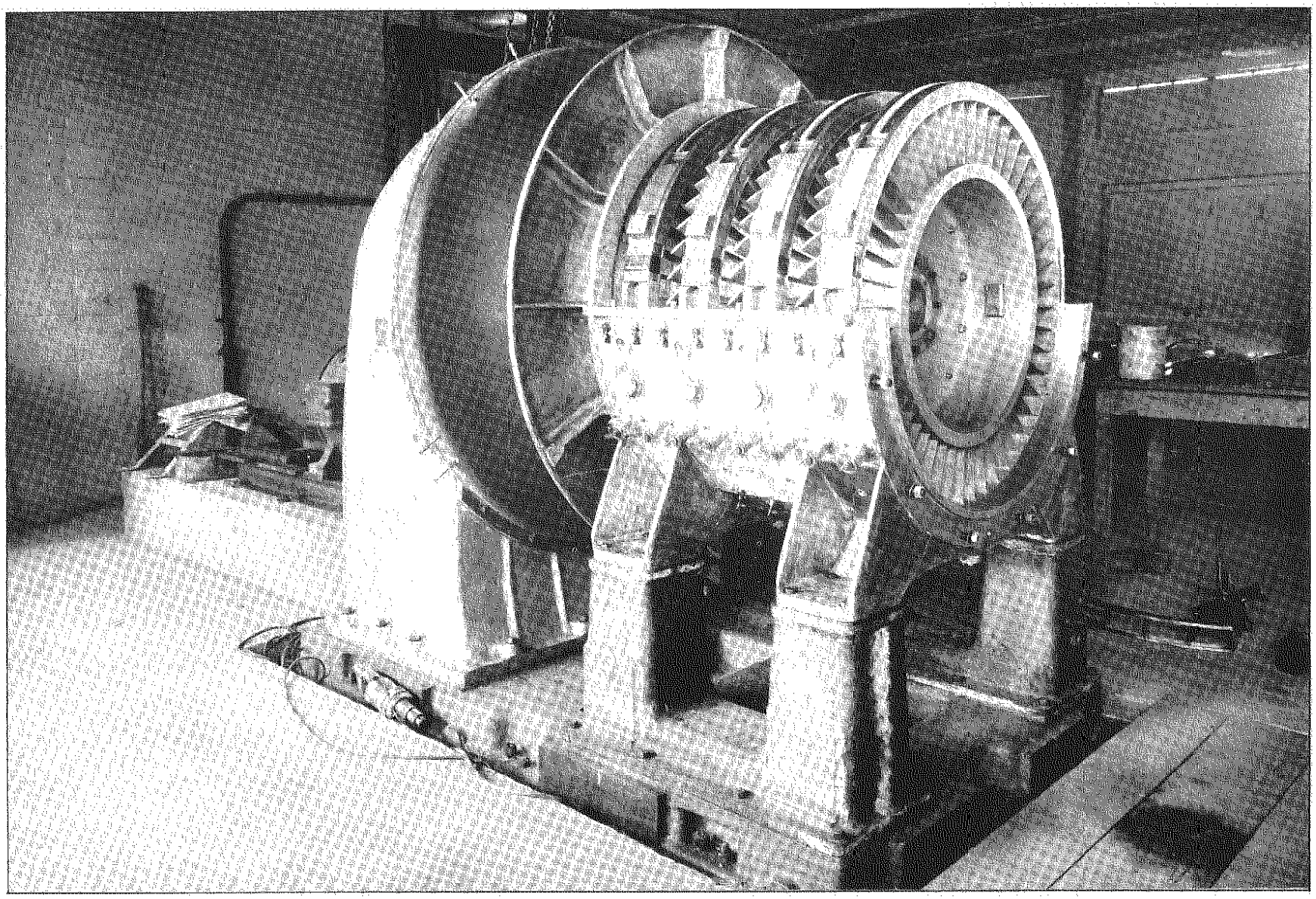

VIEW DURING ERECTION SHOWING STATOR TRAVERSING RING.

FIG. 3

FIG. 4

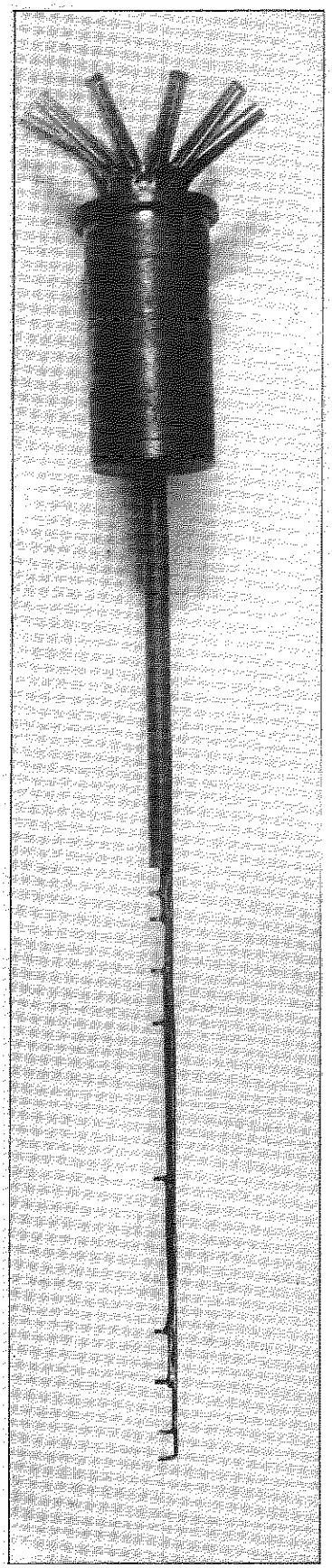

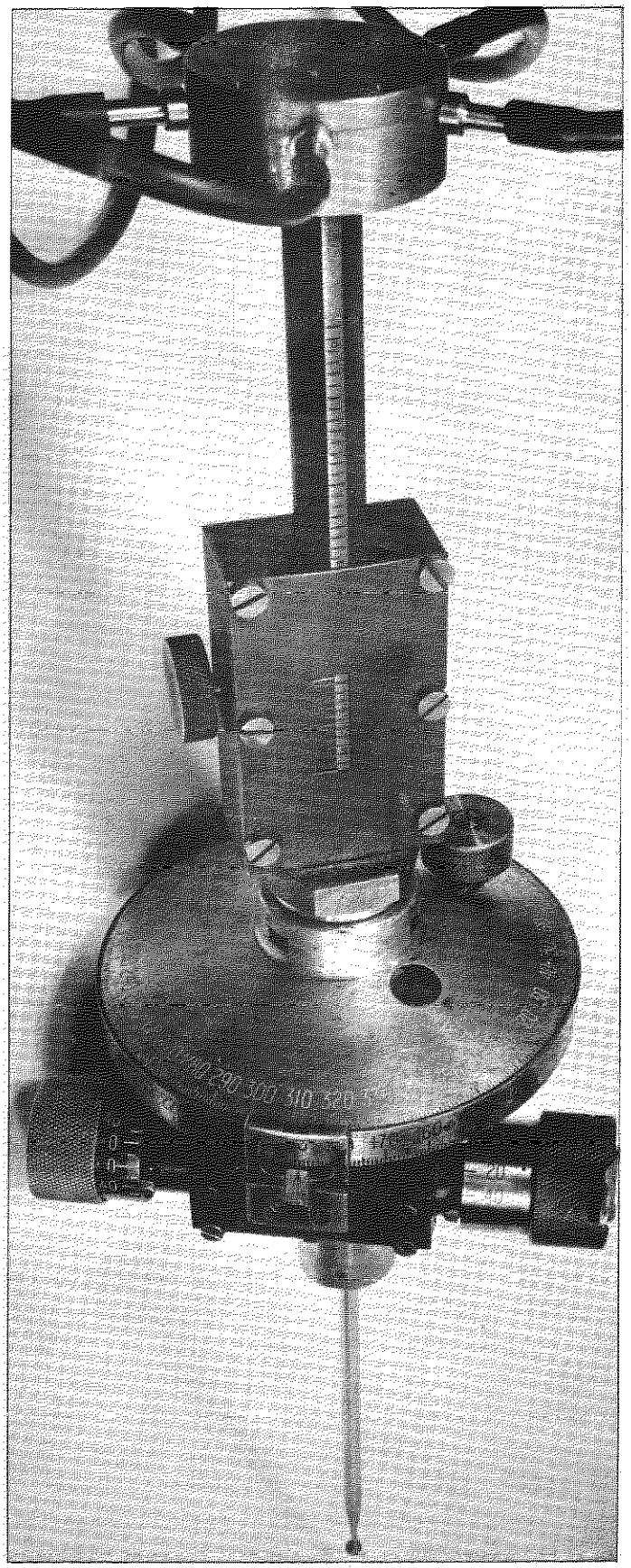

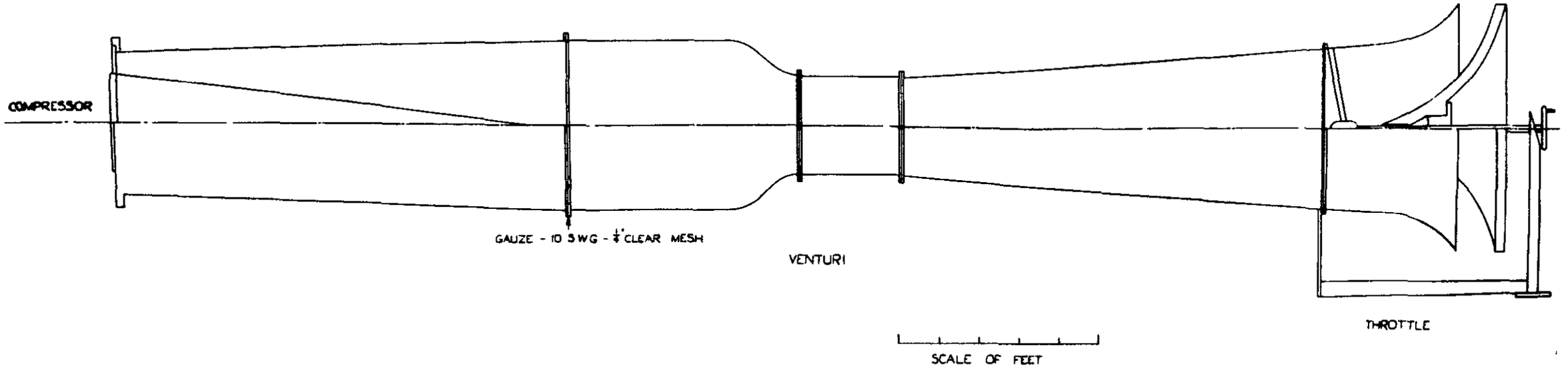

OUTLET DUCTING ARRANGEMENT.

FIG.5

FIG. 6

+ BEFORE AND AFTER INLET GUIDE VANES
○ BEFORE AND AFTER STATOR 1
□ BEFORE AND AFTER STATOR 2
△ BEFORE AND AFTER STATOR 3

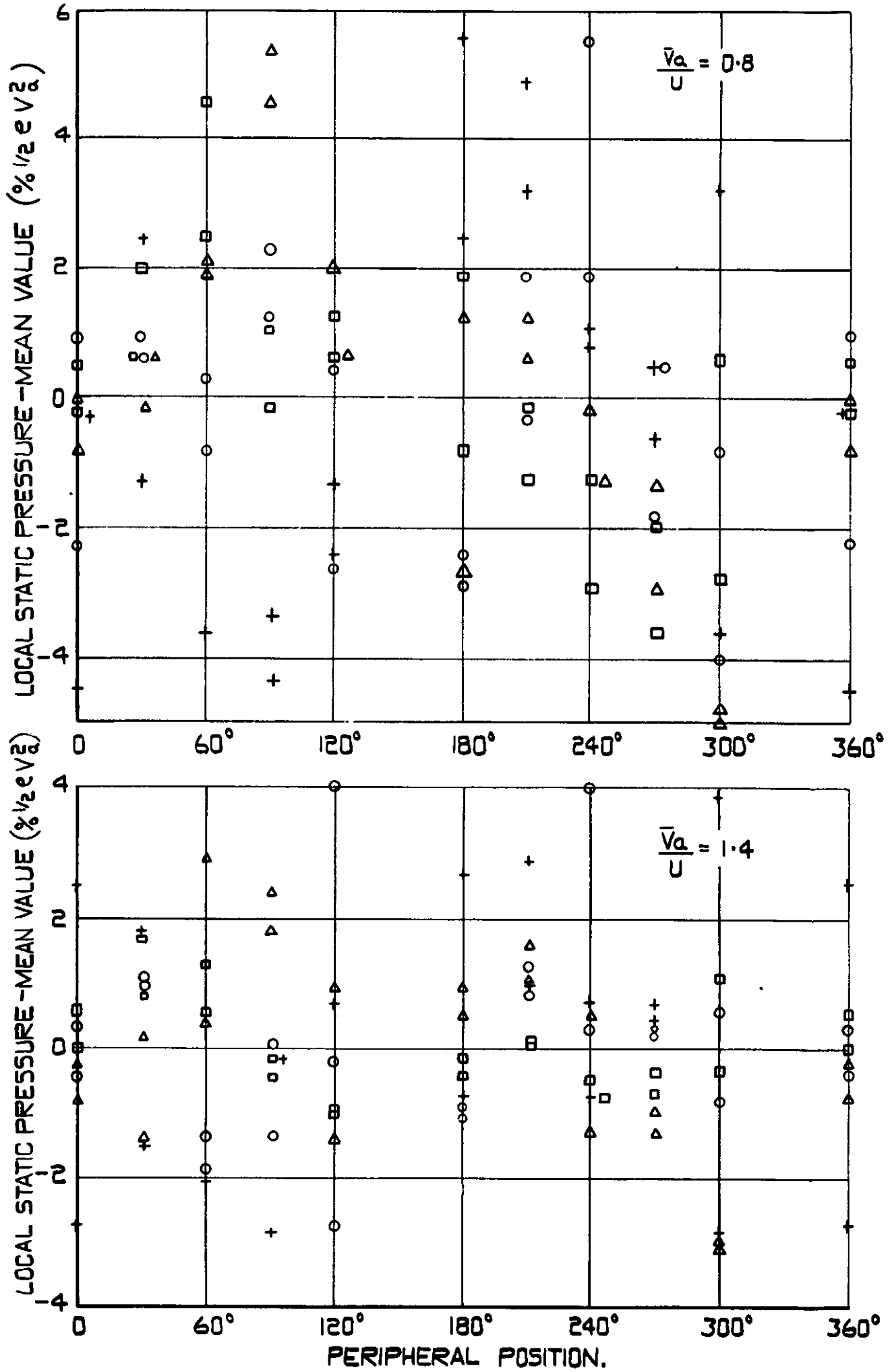

SCATTER OF COMPRESSOR STATIC PRESSURE READINGS.

FIG. 7 & 8

FIG. 7

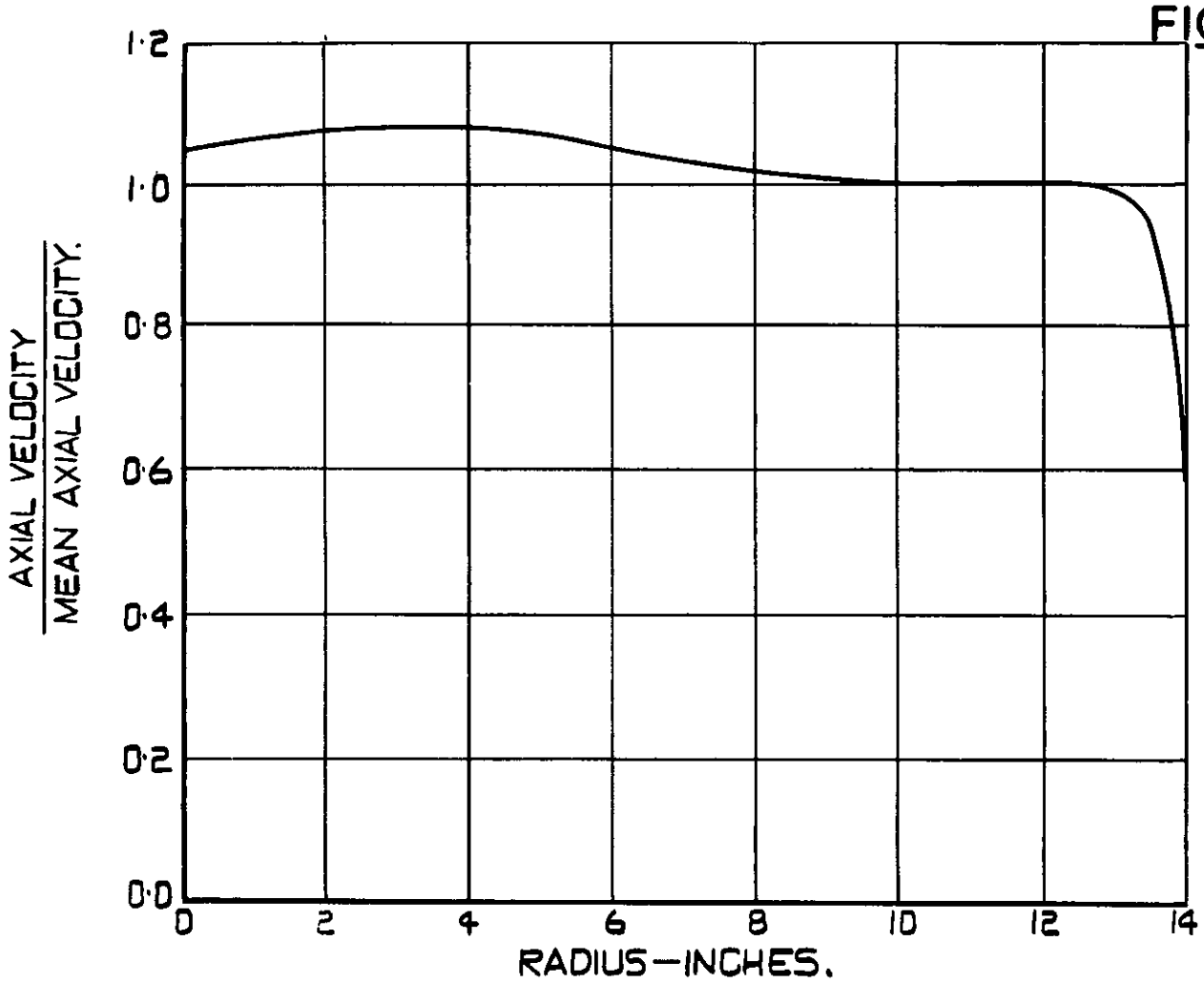

VENTURI THROAT VELOCITY PROFILE.

FIG. 8

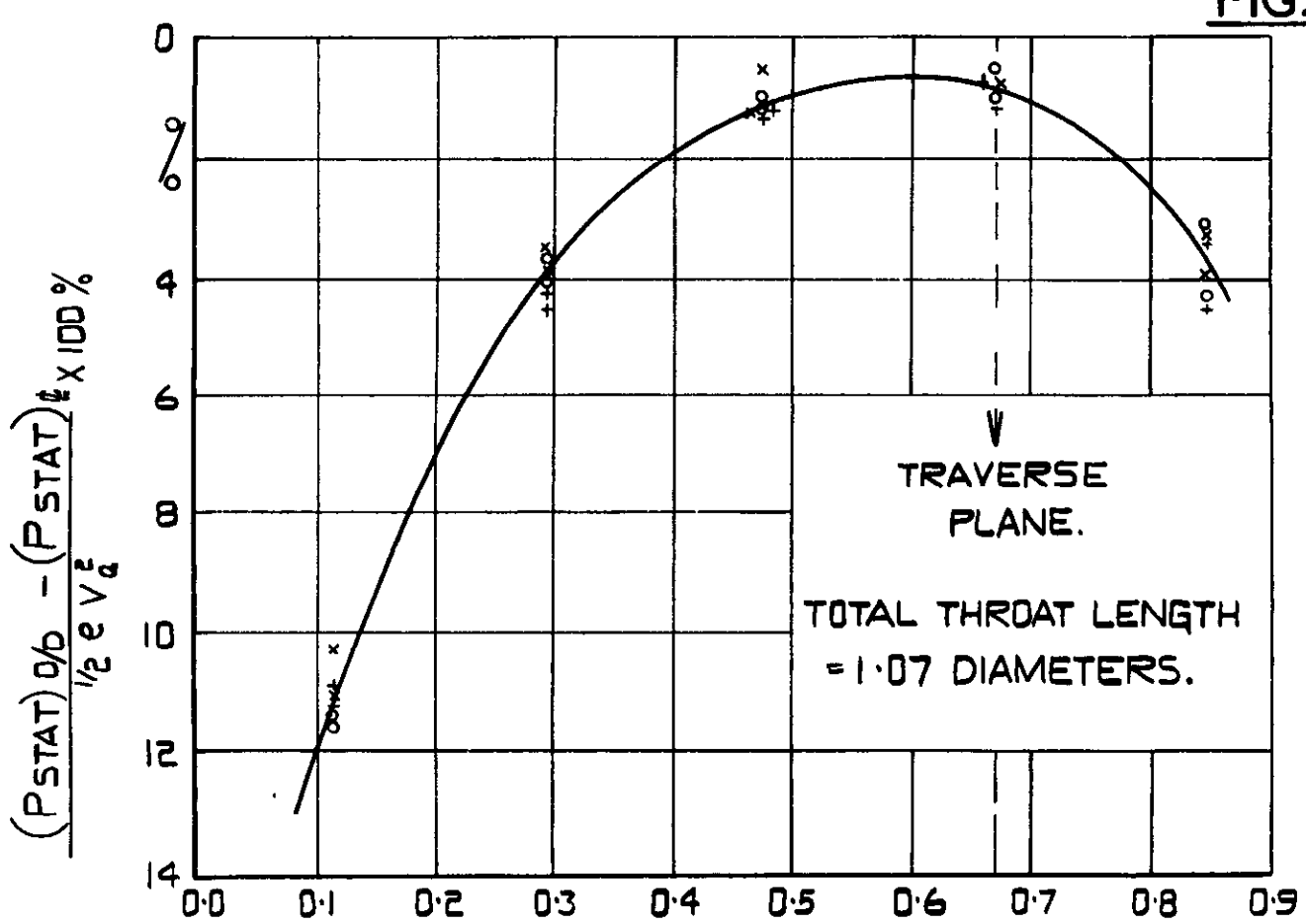

VENTURI THROAT AXIAL STATIC PRESSURE DISTRIBUTION.

FIG. 9

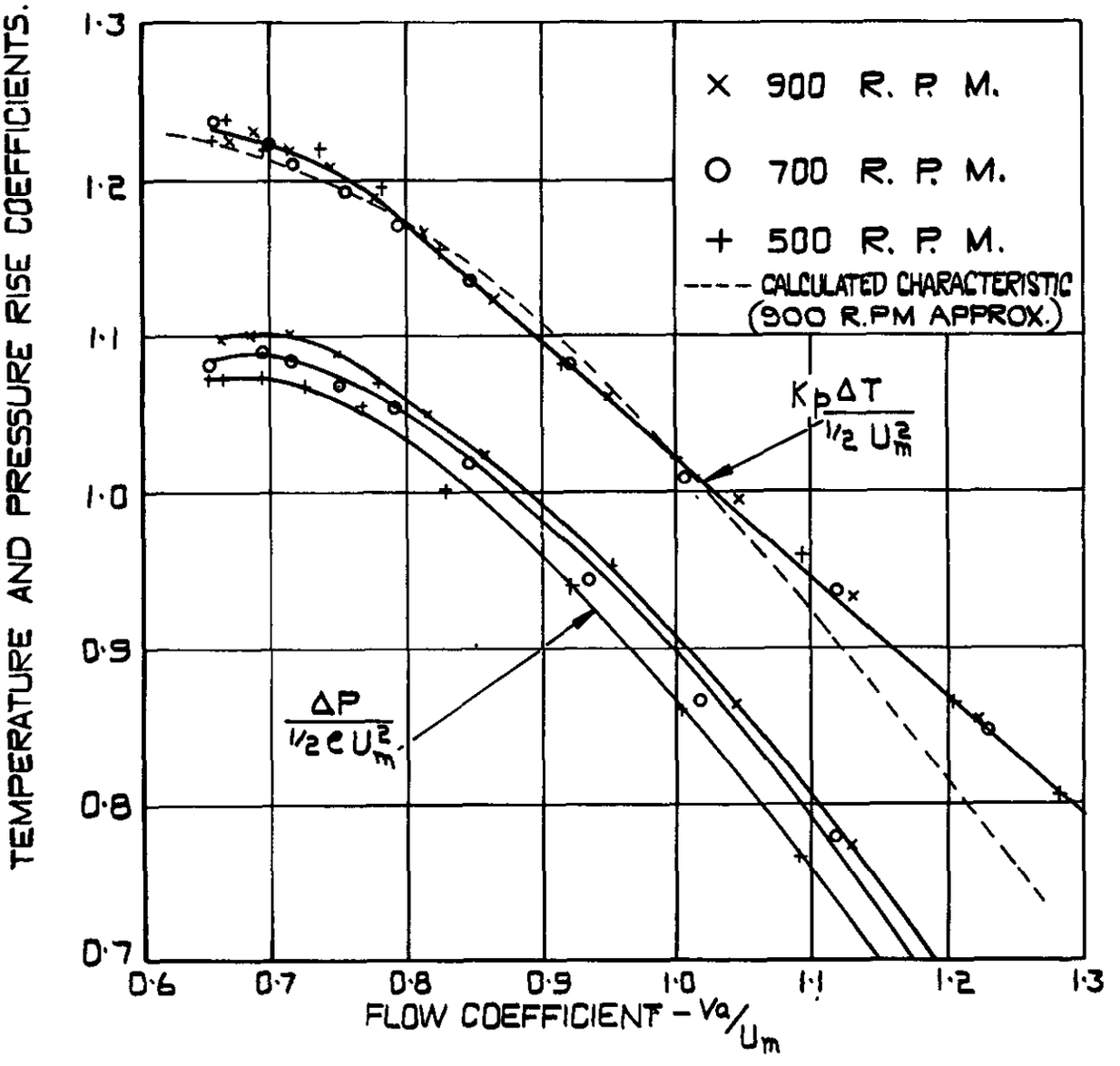

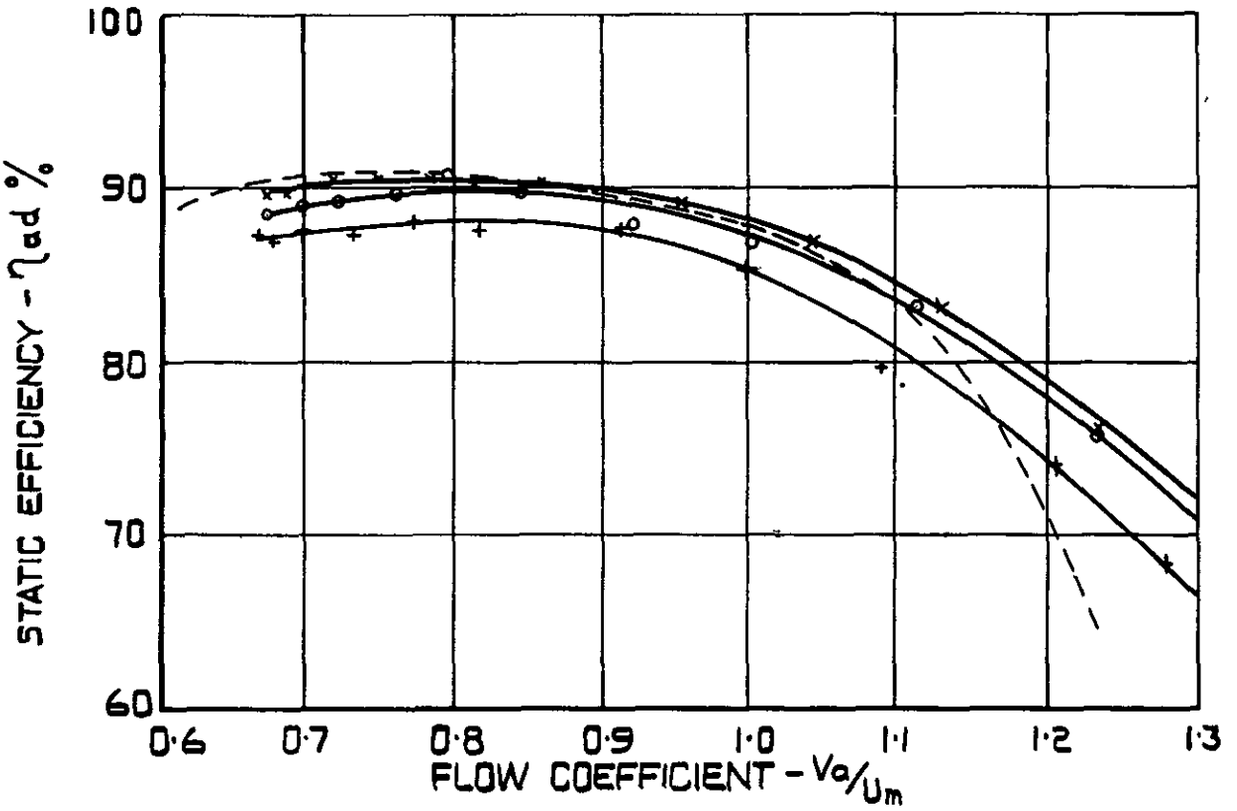

MEAN STAGE CHARACTERISTICS

WITH INLET GUIDE VANES.

FIG. 10

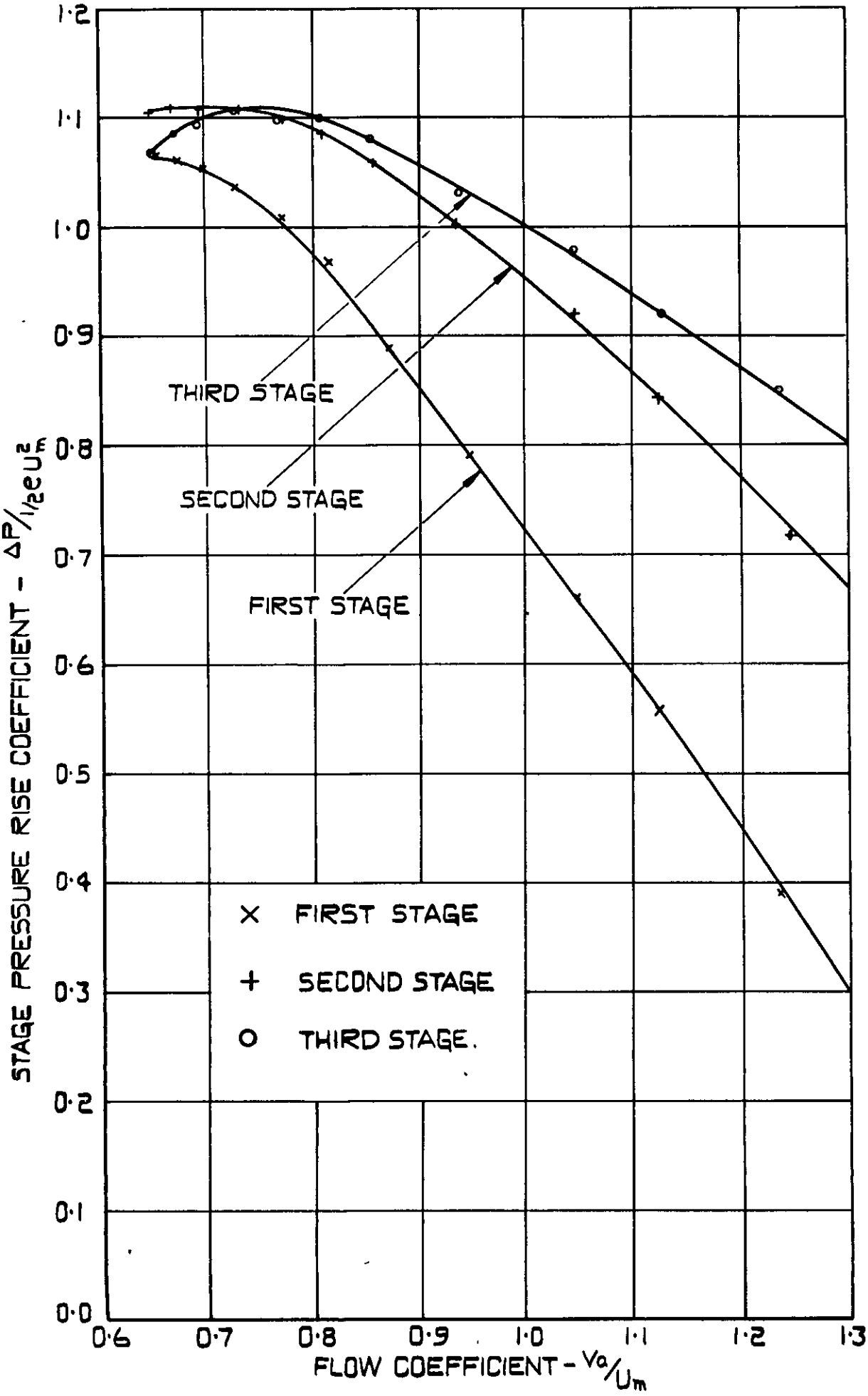

STAGE STATIC PRESSURE RISE CHARACTERISTICS

WITH INLET GUIDE VANES

700 R.P.M.

FIG. 11 & 12

FIG. 11.

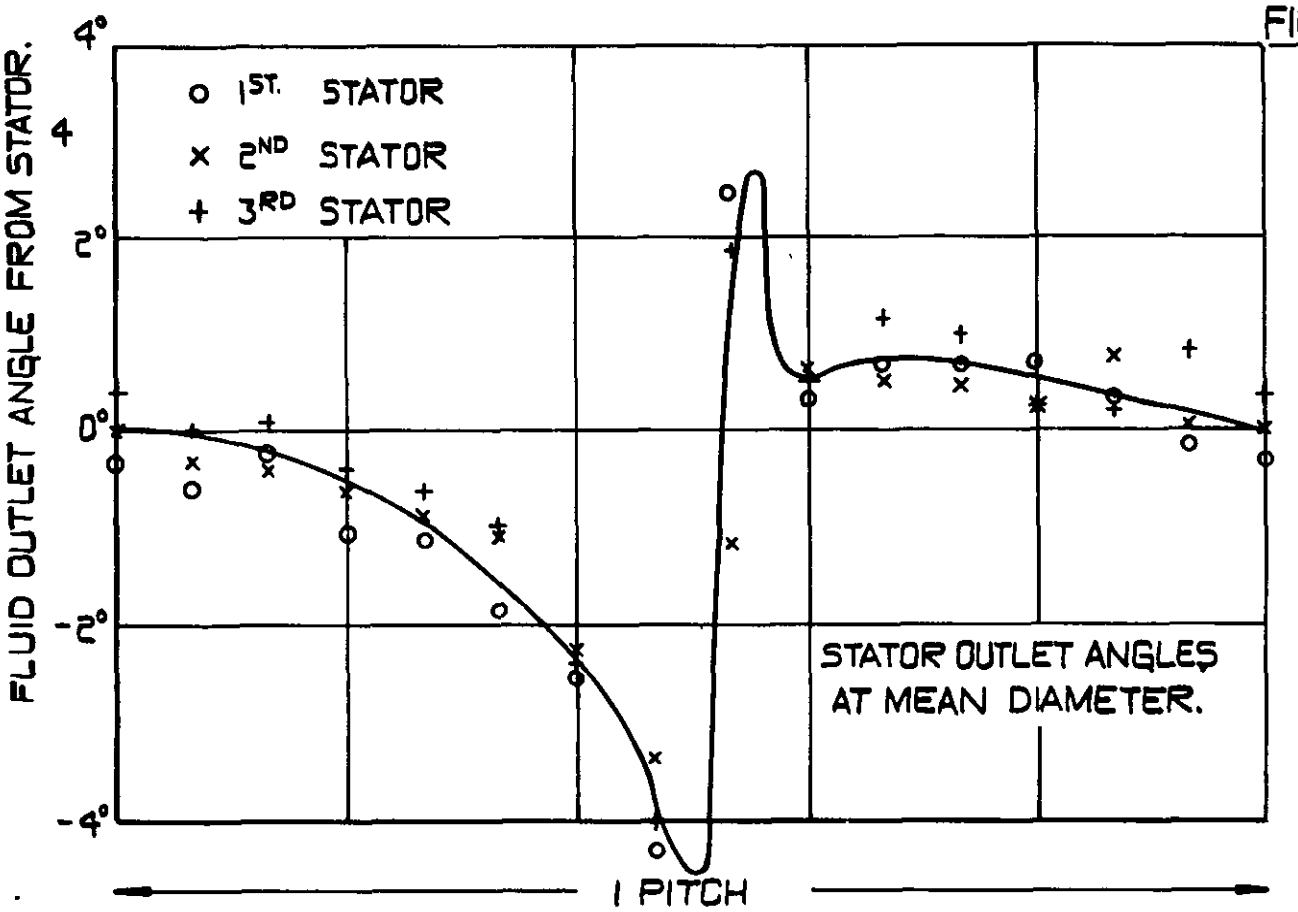

FIG. 12

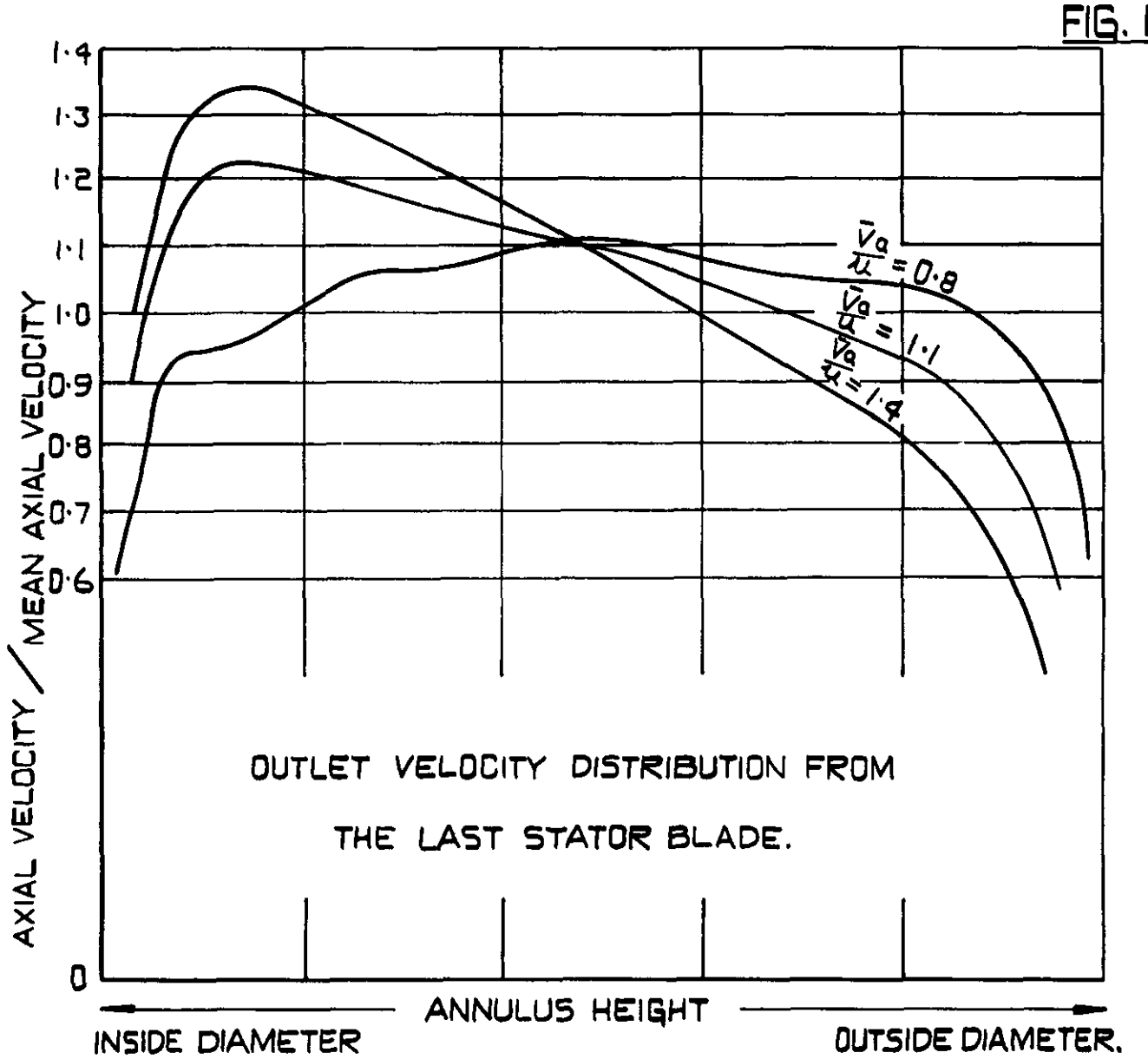

OUTLET CONDITIONS AT DESIGN POINT.

FIG. 13

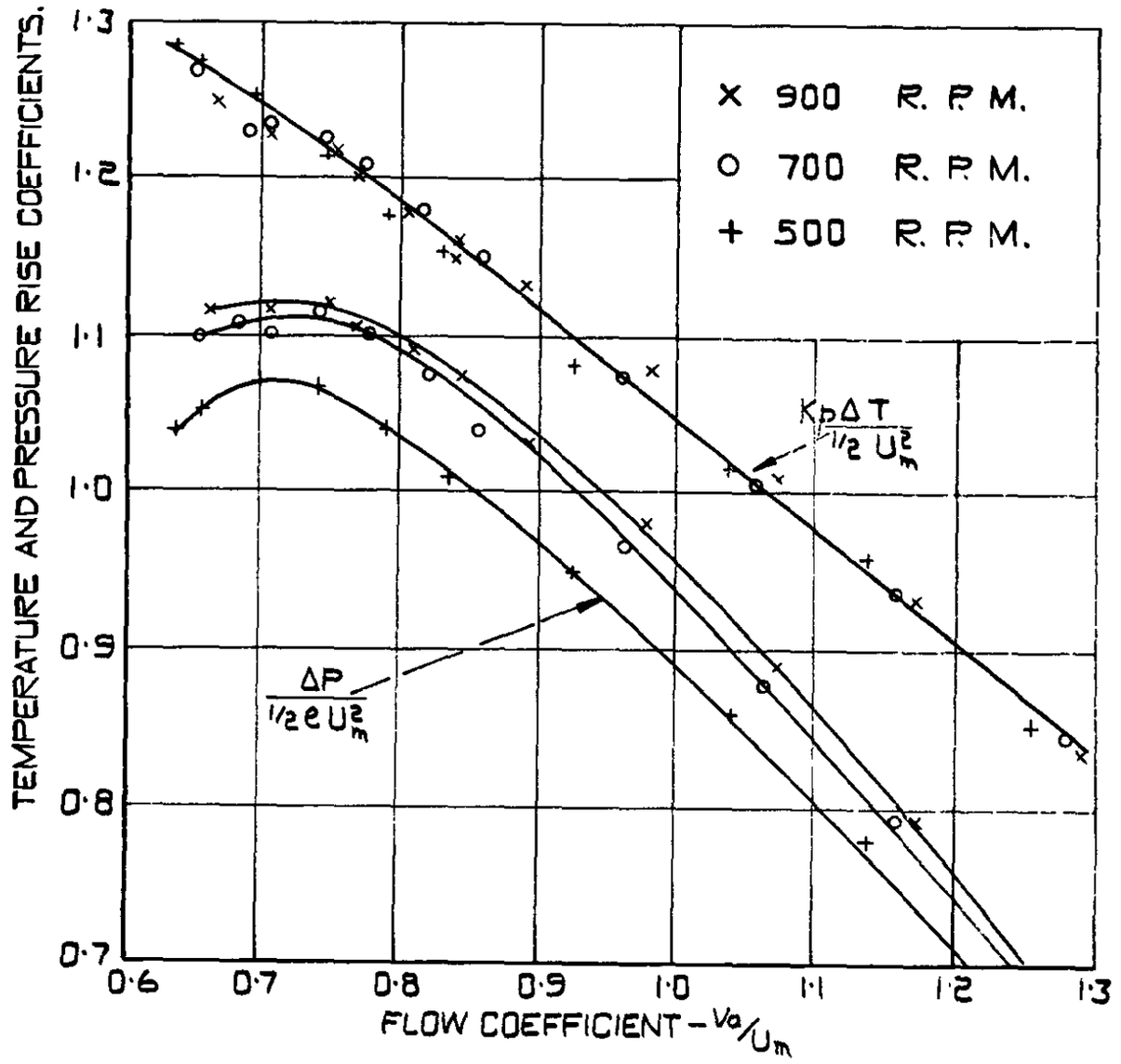

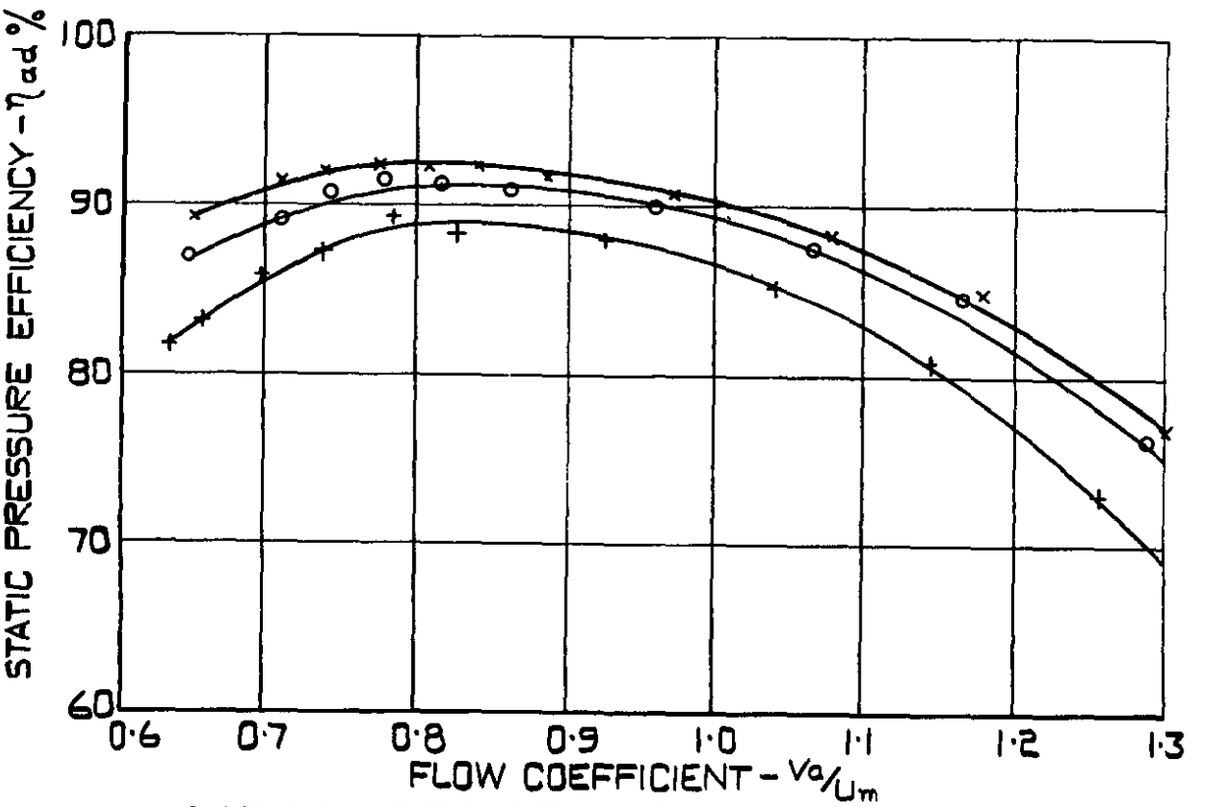

MEAN STAGE CHARACTERISTICS WITHOUT INLET GUIDE VANES.

FIG.14

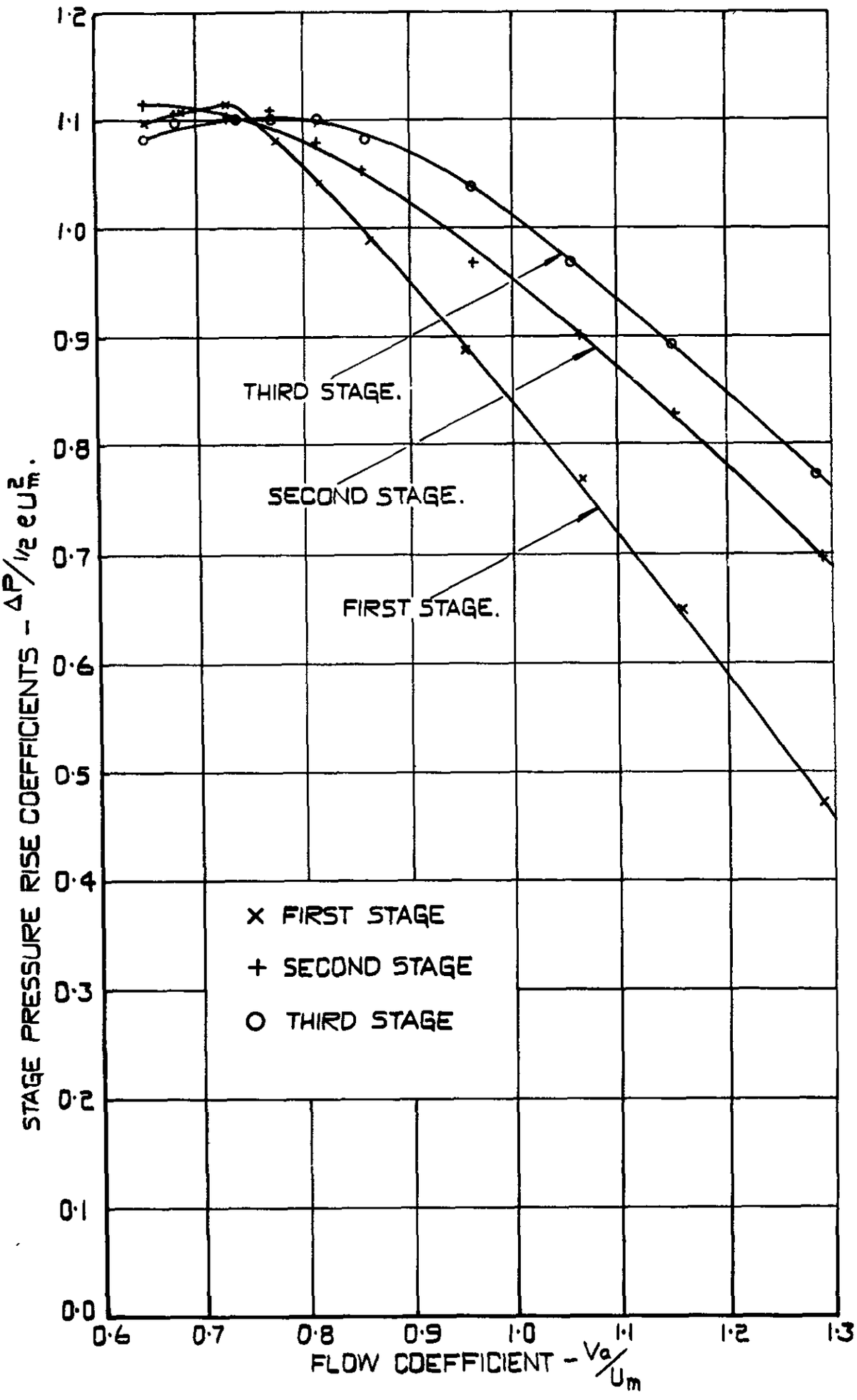

STAGE STATIC PRESSURE RISE CHARACTERISTICS

WITHOUT INLET GUIDE VANES

700 R.P.M.

FIG. 15

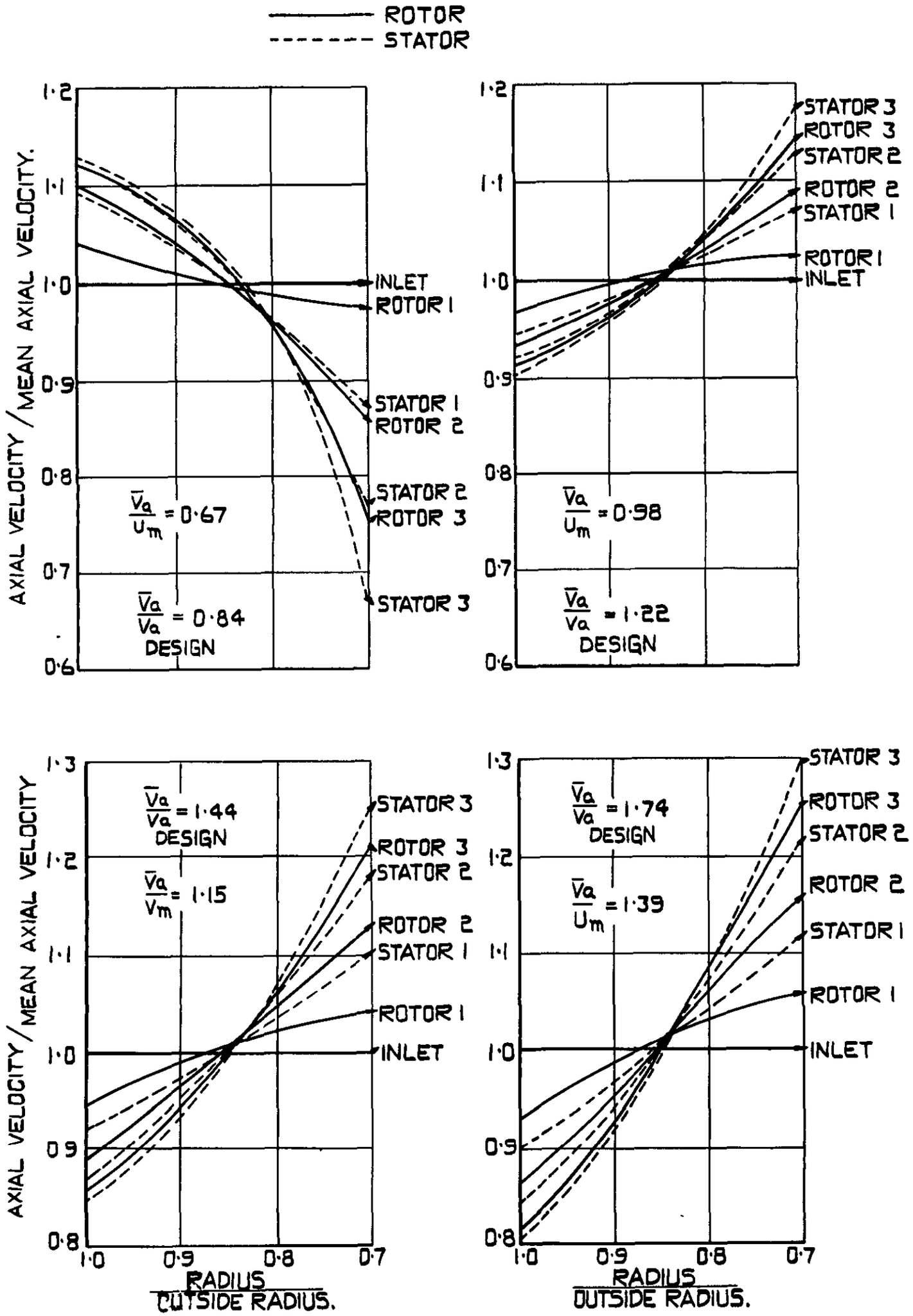

RADIAL EQUILIBRIUM VELOCITY PROFILES BETWEEN BLADE ROWS.

FIG.16

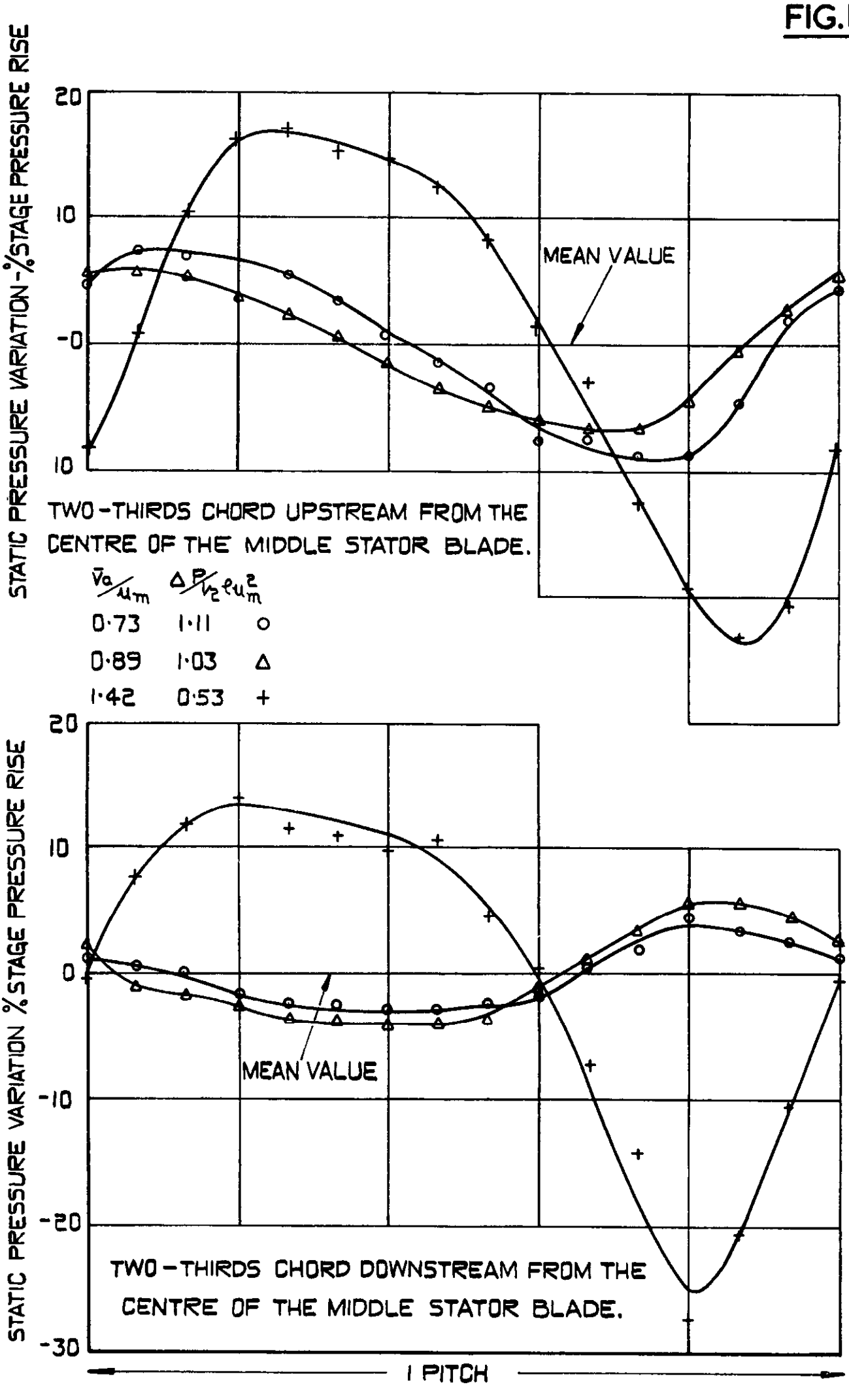

VARIATION OF MEASURED STATIC PRESSURE WITH BLADE POSITION.

FIG. 17

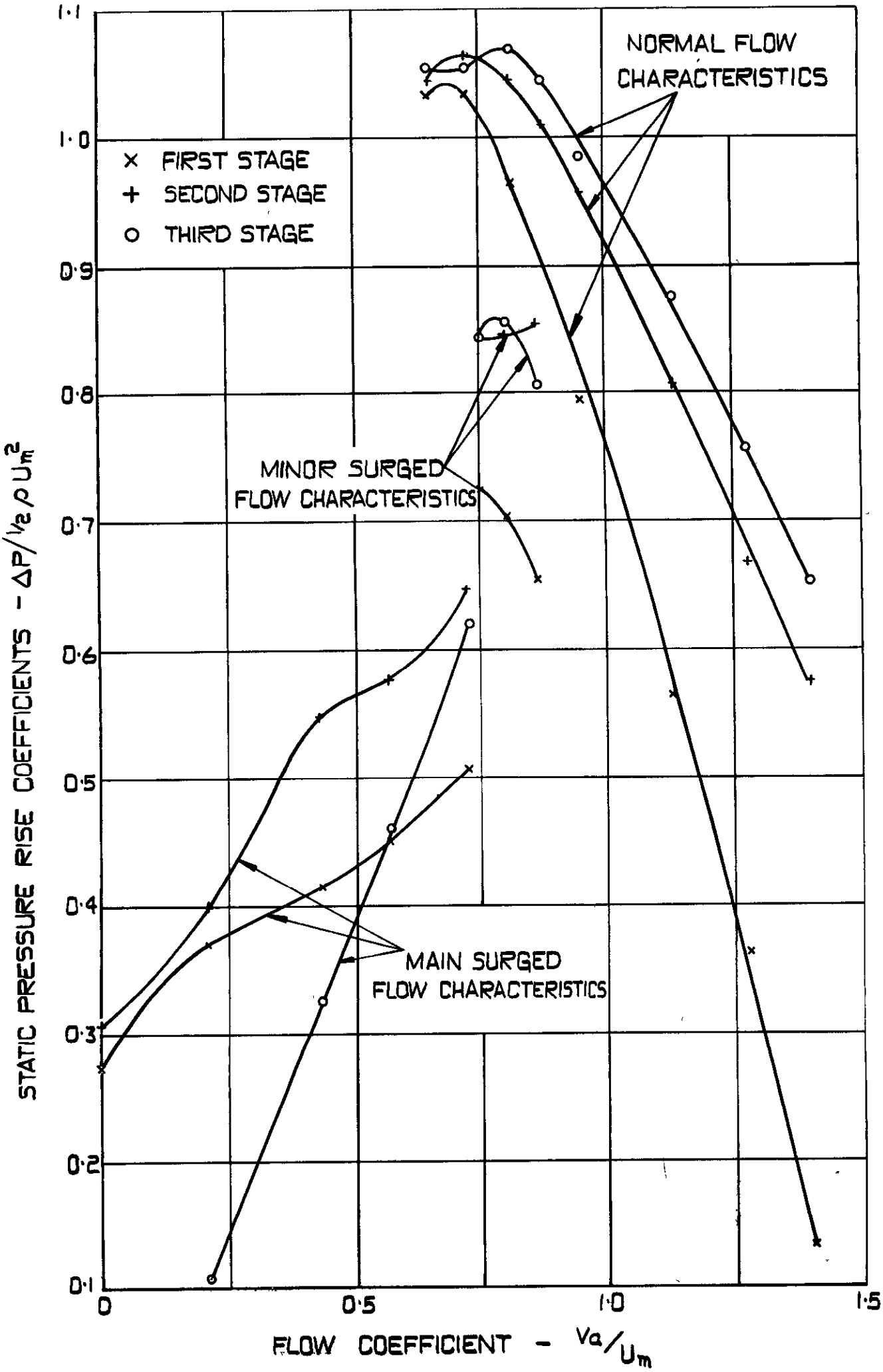

DISTRIBUTION OF STATIC PRESSURE RISE BETWEEN BLADE ROWS WHEN SURGED 500 R.P.M.

FIG. 18

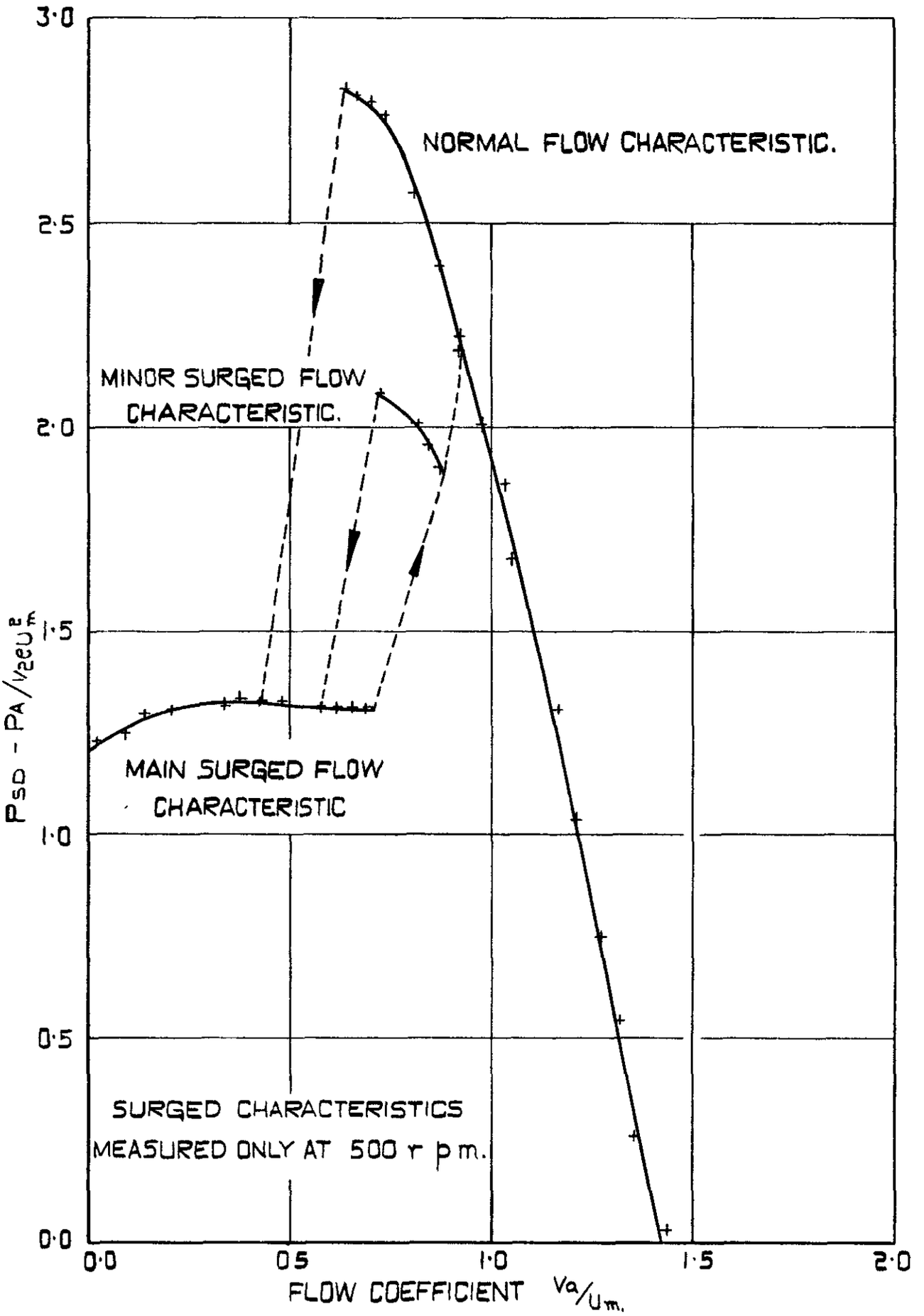

PRESSURE RISE AT THE OUTLET OF THE ANNULAR DIFFUSER.

C.P. No. 144
(15,144)
A R.C. Technical Report

CROWN COPYRIGHT RESERVED

PRINTED AND PUBLISHED BY HER MAJESTY'S STATIONERY OFFICE
To be purchased from
York House, Kingsway, LONDON, W.C.2 423 Oxford Street, LONDON, W.1
P.O. Box 569, LONDON, S.E.1
13a Castle Street, EDINBURGH, 2 1 St Andrew's Crescent, CARDIFF
39 King Street, MANCHESTER, 2 Tower Lane, BRISTOL, 1
2 Edmund Street, BIRMINGHAM, 3 80 Chichester Street, BELFAST
or from any Bookseller
1954
Price 3s 6d net
PRINTED IN GREAT BRITAIN

S O Code No 23-9007-44